CHAPTER 3

THERMODYNAMICS AND HYDRODYNAMICS OF ^{3}He–^{4}He MIXTURES

BY

A.Th.A.M. de WAELE

Low Temperature Physics Group, Department of Physics, Eindhoven University of Technology, Eindhoven, The Netherlands*

and

J.G.M. KUERTEN

Department of Applied Mathematics, University of Twente, Enschede, The Netherlands

• Partly supported by the "Stichting FOM" (Foundation for Fundamental Research on Matter), which in turn is sponsored by NWO (Dutch Organisation for the Advancement of Research).

Progress in Low Temperature Physics, Volume XIII
Edited by D.F. Brewer

Contents

1. Introduction

1.1. *Historical and scientific context*

In 1908, for the first time natural helium was liquefied by Kamerlingh Onnes (1908). About thirty years later, in 1939, it was discovered that helium has two stable isotopes: ^{4}He and ^{3}He (Alvares and Cornog 1939). Natural helium contains about 10–140 ppm ^{3}He. After the Second World War the investigation of ^{3}He and ^{3}He–^{4}He mixtures at low temperatures was started. In the pioneering period, mixtures of ^{3}He and ^{4}He, with a few percent ^{3}He content, were obtained by enriching natural helium (Beenakker and Taconis 1955). The first ^{3}He from nuclear reactions became available in 1948 (Abraham et al. 1950). This led to an intensified investigation of pure ^{3}He and ^{3}He–^{4}He mixtures.

The first review in *Progress in Low Temperature Physics* on the properties of mixtures was given in 1955 by Beenakker and Taconis. At that time many of the mixture properties were not well understood. By the time of the second review by Taconis and de Bruyn Ouboter (1964) many more aspects were fairly well understood, although the existence of a tricritical point in the ^{3}He–^{4}He phase diagram (Cohen and van Leeuwen 1960) and the finite solubility at absolute zero (Edwards and Daunt 1961, Edwards et al. 1965) were well established only (shortly) afterwards. Especially, the latter discovery opened the way to new areas of low-temperature research and to the important application in dilution refrigeration (London 1951, London et al. 1962).

The experimental properties of pure ^{3}He and dilute solutions of ^{3}He in superfluid ^{4}He at very low temperatures, with special attention to dilution refrigerators, were reviewed by Wheatley (1970).

In the above paragraphs reference is made only to general reviews of ^{3}He–^{4}He properties in *Progress in Low Temperature Physics*. Other reviews are written by Radebaugh (1967), Peshkov (1968), Ebner and Edwards (1971), Ghozlan and Varoquaux (1979), Bashkin and Meyerovich (1981), and Donnelly (1987). Books containing important chapters on ^{3}He–^{4}He mixtures are written (or edited) by Wilks (1967), Keller (1969), Lounasmaa (1974), Armitage and Farquhar (1975), Betts (1976), Ruvalds and Regge (1978), and Baym and Pethick (1978).

The developments in the understanding of ^{3}He–^{4}He mixtures in the seventies and the eighties took place in the microscopic description, and

along the lines of thermodynamics, hydrodynamics, sounds and the associated dissipative effects, convection, phenomena near the lambda line and the tricritical point, thin films, and spin-polarized systems. Furthermore, the better understanding of the mixture led to the perfection of dilution refrigerators.

The physics of ^{3}He–^{4}He solutions is too extensive to be covered by one single review. This chapter will deal with the thermodynamics and hydrodynamics of the bulk liquid at low temperatures and zero pressure. We will now give a summary of recent papers and reviews which are related to this subject, but not treated here. We hope that this may serve as a guide for further reading.

Recent papers concerning the microscopic aspects of ^{3}He–^{4}He mixtures are written by Jackson (1982), Pfitzer (1985), Hsu and Pines (1985), Fabrocini (1986), de Bruyn Ouboter and Yang (1987), Sridhar and Shanthi (1987), Dalfovo and Stringari (1988), Pang (1988), Singh (1988), and Devreese et al. (1989). Adamenko and Rudavskii (1987) have reviewed the kinetics of the phonon–impurity system of ^{3}He–^{4}He superfluid solutions. Work regarding the various types of sounds is reported by Fujii et al. (1986), Lea et al. (1987), Wiegers et al. (1988), and Adamenko et al. (1988). Recent papers on thermal convection are written by Fetter (1982), Ecke et al. (1987), Bloodworth et al. (1987), and Ardron et al. (1987). Meyer (1988) has reviewed the transport properties near the lambda line and the tricritical point. The properties of spin-polarized ^{3}He–^{4}He mixtures have been reviewed by Meyerovich (1987). Properties of thin films have recently been described by Laheurte et al. (1987), Papoular and Romagnan (1987), Krotscheck et al. (1988) and Valles et al. (1988).

1.2. *Outline*

The specific heat of liquid ^{3}He–^{4}He mixtures is usually written in terms of the sum of the specific heat of a ^{3}He-quasiparticle gas and the specific heat of the pure ^{4}He component. In sect. 2 the thermodynamics based on this starting point is derived. Relations of important quantities and their low- and high-temperature limits are given. These are used to derive expressions for the velocity of second sound. This latter quantity is a very important source of information for the Fermi gas properties. The work in this field is critically reviewed. Finally, the Fermi gas parameters are summarized.

In sect. 3 the experimental aspects of the ^{3}He–^{4}He hydrodynamics are treated. The appearance of mutual friction, which has long been neglected in this field, is discussed, together with the properties of the critical velocities. The phenomenological equations of motion are given. Attention is paid to the experimental results in the 0.7 to 2 K region, where the rotons and

phonons play an important role, and to the temperature region below 250 mK, where the ^{4}He excitations can be neglected.

The occurrence of mutual friction is a strong indication that ^{4}He vortices play an important role in ^{3}He–^{4}He hydrodynamics. In sect. 4 first the hydrodynamic expressions are derived from the thermodynamics of irreversible processes, along the lines of Khalatnikov (1965), and de Groot and Mazur (1962). From the equation of motion of quantized ^{4}He vortices, the observed cubic velocity dependence of the ^{4}He chemical potential difference is explained on purely dimensional grounds. A differential equation is given from which the temperature profile (and the profiles of the pressure and ^{3}He concentration) in a cylindrical tube in which ^{3}He flows through superfluid ^{4}He, can be calculated.

In sect. 5 the results of the previous sections are applied to dilution refrigerators. It is emphasized that, on the one hand, mutual friction can degrade the performance of these machines but, on the other hand, that it is *essential* for their proper operation: in ^{3}He-circulating refrigerators mutual friction prevents the formation of a destabilizing superfluid "plug" at the concentrated side. In ^{4}He-circulating machines the ^{3}He circulates internally between the mixing chamber and the demixing chamber under the action of mutual friction. Especially, in the latter case mutual friction plays an essential role in the proper operation of the machine.

In the last section we compare the ^{3}He–^{4}He hydrodynamics with the hydrodynamics in pure ^{4}He-II and discuss our point of view on the state of affairs in ^{3}He–^{4}He thermodynamics and hydrodynamics.

2. Thermodynamics of ^{3}He–^{4}He mixtures

2.1. *Introduction*

In this section we derive the expressions for thermodynamic functions of state of ^{3}He–^{4}He-II mixtures at zero pressure, and related quantities such as the osmotic pressure and the velocity of second sound.

The specific heat of liquid ^{3}He–^{4}He mixtures is often treated as the sum of a ^{4}He contribution and a ^{3}He contribution. The ^{4}He is superfluid whereas the ^{3}He behaves as a gas of quasiparticles. We derive relations which follow immediately from this separation of the specific heat. In the next section it is assumed that the quasiparticles are Fermi particles with an excitation spectrum which is nearly quadratic. The deviations of the quadratic spectrum are small and are treated in a first-order approximation. Therefore, we will call the gas a *nearly* ideal Fermi gas. At present, the ^{3}He contribution to the

specific heat, second sound, osmotic pressure, etc. are usually described with this model.

Relations are derived which are valid at all temperatures. These relations serve as the basis for deriving expressions in the low-temperature and high-temperature limits, which are of practical importance e.g. for the interpretation of the measurements of the specific heat and second sound of dilute mixtures. In our view a consistent derivation is necessary because some derivations in the literature are inconsistent. Finally, recent experimental results of the thermodynamic properties of ^{3}He–^{4}He mixtures, interpreted in the framework of the nearly ideal gas, are shortly reviewed.

Many aspects of the expressions for thermodynamic quantities of ^{3}He–^{4}He mixtures given in this chapter are presented before by other authors, e.g. by Radebaugh (1967), Ebner and Edwards (1971), Disatnik and Brucker (1972), Ghozlan and Varoquaux (1979), Greywall (1979), Corruccini (1984), Kuerten et al. (1985a, b), Bowley (1985) and Owers–Bradley et al. (1987).

2.2. *The quasiparticle description*

We start our discussion of the thermodynamics of ^{3}He–^{4}He-II mixtures by writing the molar specific heat of the mixture C_m as

$$C_m(T, x) = xC(^3\text{He}) + (1-x)C(^4\text{He}), \tag{1}$$

with

$$C(^3\text{He}) = C_q(T, x) \tag{2}$$

and

$$C(^4\text{He}) = C_4^0(T). \tag{3}$$

In these equations x is the molar ^{3}He concentration, C_4^0 is the molar specific heat of pure ^{4}He at constant volume and C_q is the specific heat of a quasiparticle gas at the same particle density as the ^{3}He component. In this section we do not specify the nature of the quasiparticles. Equations (1)–(3) can be regarded as defining C_q. The model in which the quasiparticles are treated as a nearly ideal Fermi gas is introduced in the next section.

In general, the superscript 0 refers to a pure substance. The subscripts 3 and 4 refer to ^{3}He and ^{4}He, respectively. Quantities corresponding to the quasiparticles in general have been represented by a lower index q. In the case the quasiparticle gas is considered as an *ideal* Fermi gas the quantities carry a lower index F. The corresponding quantities for the *nearly* ideal Fermi gas are denoted with an additional prime. In general, the variables of functions are written explicitly only when the function is introduced for the first time, or

when it is of particular importance for the understanding of the derivation. As the discussion is limited to the fluid properties at zero pressure, the pressure dependencies will not be given explicitly, except for the relations where the osmotic pressure is introduced.

The entropy of the solution S_m can be calculated as a function of T and x by a single integration of C_m/T at constant x from $T=0$ to T, since according to the third law S_m at 0 K is independent of x. We put the entropies at 0 K equal to zero. The result is:

$$S_m(T, x)=xS_q(T, x)+(1-x)S_4^0(T)\,, \tag{4}$$

where S_4^0 is the molar entropy of pure ^{4}He, and S_q represents the entropy of the quasiparticles. We like to point out that no term with $-x\ln(x)-(1-x)\ln(1-x)$ (the classical entropy of mixing) should be added to S_m (Greywall 1979, Husson et al. 1983).

The internal energy U_m can be obtained from eqs. (1)–(3) by integration over T, and gives

$$\begin{aligned} U_m(T, x)=U_m(0, x)&+x[U_q(T, x)-U_q(0, x)] \\ &+(1-x)[U_4^0(T)-U_4^0(0)], \end{aligned} \tag{5}$$

where U_q and U_4^0 represent the internal energies of the quasiparticle gas and pure ^{4}He, respectively.

From eqs. (4) and (5) only differences between thermodynamic quantities at temperature T and $T=0$ at a given concentration can be calculated. In the specification of the properties of the quasiparticles we still have to fix $U_q(0, x)$, the zero level of the energy. It will be taken in such a way that

$$U_m(0, x)=xU_q(0, x)+(1-x)U_4^0(0). \tag{6}$$

This means that eq. (5) assumes the form

$$U_m(T, x)=xU_q(T, x)+(1-x)U_4^0(T). \tag{7}$$

We will take the internal energies of the pure components at 0 K to be equal to zero: $U_3^0(0)=0$ and $U_4^0(0)=0$. In this case

$$U_m(0, x)=U_m^E(0, x), \tag{8}$$

where U_m^E is the excess internal energy per mole solution.

The molar volume V_m is given by

$$V_m(x)=V_4^0(1+x\alpha), \tag{9}$$

where V_4^0 is the volume per mole of pure ^{4}He and α is a constant (Bardeen et al. 1967). The molar volume V_m will be considered to be pressure- and temperature-independent.

The molar Gibbs free energy G_m follows from $G_m = U_m + pV_m - TS_m$. The ^{4}He chemical potential follows from

$$\mu_4 = G_m - x\left(\frac{\partial G_m}{\partial x}\right)_T. \tag{10}$$

Substituting eqs. (4), (6) and (7) gives

$$\mu_4(T, x) = G_4^0(T) - x^2\left(\frac{\partial F_q(T, x)}{\partial x}\right)_T, \tag{11}$$

where G_4^0 is the Gibbs free energy of pure ^{4}He and F_q is the free energy of the quasiparticle gas. The last term in eq. (11) can be written as

$$x^2\left(\frac{\partial F_q}{\partial x}\right)_T = p_q(T, x)V_4^0, \tag{12}$$

where we have used the relations $\partial F_q/\partial x = (\partial F_q/\partial V)(dV/dx)$ and $(\partial F_q/\partial V)_T = -p_q$. In these relations p_q is the pressure of the quasiparticle gas at the same particle density as the ^{3}He component. Furthermore,

$$V = V_m/x \tag{13}$$

is the volume per mole ^{3}He. From eqs. (11) and (12) it follows that

$$\mu_4(T, x) = G_4^0(T) - p_q(T, x)V_4^0. \tag{14}$$

Equation (14) implies that the chemical potential of pure ^{4}He at zero pressure is equal to the ^{4}He chemical potential in the solution at a pressure p_q.

In the thermodynamics and the hydrodynamics of mixtures the osmotic pressure Π plays a central role. It can be defined in two equivalent ways:

$$\Pi(\mu_4, T, x) = p(\mu_4, T, x) - p(\mu_4, T, 0) \tag{15}$$

or

$$\mu_4(p, T, x) = G_4^0(p - \Pi, T). \tag{16}$$

In eq. (16) we have written the pressure dependence of the chemical potential explicitly. At low values of p, T and x the right-hand side can be expanded to first order, yielding

$$\mu_4(p, T, x) = G_4^0(p, T) - \Pi(T, x)V_4^0. \tag{17}$$

Comparing eq. (14) with eq. (17) shows that the osmotic pressure can be identified with the pressure of the quasiparticle gas:

$$\Pi(T, x) = p_q(T, x). \tag{18}$$

In a similar way an expression for μ_3 can be derived resulting in

$$\mu_3(T, x) = G_q(T, x) - p_q(T, x)V_3. \tag{19}$$

The ^{3}He partial volume $V_3 = V_4^0(1+\alpha)$. Equation (19) implies that G_q is equal to the ^{3}He chemical potential μ_3 in a solution at a pressure p_q (Ebner and Edwards 1971).

Equations (17) and (19) are consistent with the Gibbs–Duhem relation

$$x\,\mathrm{d}\mu_3 + (1-x)\mathrm{d}\mu_4 = -S_m\,\mathrm{d}T + V_m\,\mathrm{d}p, \tag{20}$$

as can be verified by substitution, keeping in mind that $(\partial G_q/\partial p_q) = V$. The expressions for μ_3 and μ_4 given by Greywall (1979) and Husson et al. (1983) are not consistent with eq. (20).

Equation (20), applied at $T=0$ and $p=0$ and making use of eqs. (14) and (18) gives

$$\mu_3(0, x) = V_4^0 \int_{x_0}^{x} \frac{1-x'}{x'} \frac{\mathrm{d}\Pi_0}{\mathrm{d}x'}\,\mathrm{d}x'. \tag{21}$$

In this equation x_0 is the concentration of the dilute saturated solution at 0 K. The chemical potentials of pure ^{3}He and ^{4}He are zero at 0 K, so $\mu_3(0, x_0) = G_3^0(0) = U_3^0(0) = 0$ and $G_4^0(0) = 0$.

In eq. (21) $\Pi_0(x)$ is the osmotic pressure at 0 K. It is related to the excess internal energy through eqs. (8), (10) and (17), keeping in mind that $G_m = U_m$ at $T=0$. The osmotic pressure at nonzero temperatures, and the other thermodynamic quantities can, thus, be calculated from the excess internal energy (or the osmotic pressure at zero temperature) and the specific heat of the quasiparticle gas.

The excess enthalpy H^E is defined as

$$H^E(T, x) = H_m(T, x) - xH_3^0(T) - (1-x)H_4^0(T), \tag{22}$$

where H_m is the molar enthalpy of the solution, and H_3^0 and H_4^0 are the molar enthalpies of pure ^{3}He and ^{4}He, respectively. The excess enthalpy plays an important role in experiments where the two pure components are mixed, and in the comparison between the calculations and the experiments (Seligmann et al. 1969, Karnatsevich et al. 1984).

Conservation of energy of adiabatic ^{3}He flow through ^{4}He-II (Ebner and Edwards 1971), leads to

$$H_3^{os} = \text{constant}, \tag{23}$$

where H_3^{os} is given by

$$H_3^{os}(T, x) = \mu_3 + \frac{TS_m}{x}. \tag{24}$$

It is called the osmotic enthalpy per mole ^{3}He. For low temperatures and not too low ^{3}He concentrations the ^{4}He contribution to the entropy is negligible.

2.3. *The nearly ideal Fermi gas*

We will now introduce the assumption that the quasiparticles constitute a nearly ideal gas of Fermi particles. From this assumption relations are derived for the thermodynamic functions of state. The thermodynamics of a two-component mixture is treated in many textbooks; see e.g. Guggenheim (1967). For a detailed treatment of the thermodynamics of the ideal Fermi gas, the reader is referred to general textbooks on statistical mechanics, e.g. Huang (1987).

The separation of the mixture specific heat as represented by eqs. (1)–(3), with C_q equal to the specific heat of a Fermi gas, is based on the theory of Pomeranchuk (1949). It was shown to be correct to order x for the first time by de Bruyn Ouboter et al. (1960). In fact, there is no reason why $C(^4\text{He})$ should be absolutely independent of the ^{3}He concentration. In the mixture the ^{4}He occupies a larger volume than the same quantity of ^{4}He in the pure phase. The difference between the true ^{4}He contribution to the specific heat of the solution and the value of the pure fluid can well be of the order of $4x\alpha_p V_3^0/\kappa_T$, where α_p is the isobaric expansion coefficient of ^{4}He, V_3^0 the molar volume of pure ^{3}He, and κ_T the isothermal compressibility. For a 1% mixture at $T=0.5$ K this term is about 1% of C_m.

A concentration dependence of $C(^4\text{He})$ would affect the interpretation of $C(^3\text{He})$ in terms of the Fermi gas specific heat, and all results derived from this, such as the value of the effective mass and the form of the quasiparticle excitation spectrum. In this review we will assume the validity of eqs. (1)–(3).

In its simplest form the single-particle excitation spectrum is parabolic, as given by Landau and Pomeranchuk (1948). In this case one can apply the familiar ideal Fermi gas statistics at a given fixed concentration.

The excitation spectrum of the Fermi particles and their effective mass can be determined from measurements of the specific heat, the osmotic pressure, second sound, the normal-component density (Esel'son et al. 1976, Pogorelov et al. 1979) and neutron scattering. It turns out that the excitation spectrum of the ^{3}He quasiparticles is slightly nonparabolic (see, e.g. Ebner and Edwards 1971, Disatnik and Brucker 1972, Greywall 1979, Szprynger 1982, van der Zeeuw et al. 1984).

The relations derived in the preceding section can be applied to the nearly ideal Fermi gas. The lower index q has to be replaced by a lower index F and a prime.

To second order in k^2 the excitation spectrum is represented by

$$\varepsilon(x, k)=\varepsilon_0(x)+\varepsilon'_F(x, k), \tag{25}$$

with

$$\varepsilon'_F(x, k)=\frac{\hbar^2 k^2}{2m^*(x)}(1+\gamma k^2)\,, \tag{26}$$

where $m^*(x)$ is the quasiparticle effective mass at concentration x, k is the magnitude of the wave vector, $\hbar$ is Planck's constant divided by 2π and $\varepsilon_0(x)$ is the potential energy of the quasiparticles. The form of the excitation spectrum given by eq. (26) was proposed by Brubaker et al. (1970). The parameter γ is a measure for the nonparabolicity of the excitation spectrum. The presently accepted value is about -0.08 Å^2.

As eq. (26) is a development of ε to second order in k^2, there is no point in expressing derived quantities to higher than first order in γ. Strictly speaking, third-order terms in k^2 are of importance in view of the high accuracy of the measurements of the specific heat and the second-sound velocity. So higher-order terms should be included in the description of ^{3}He as a nearly ideal Fermi gas. In our treatment we confine the calculation to the second order in k^2. The validity of the relations is limited accordingly.

The density of states $n'_F(\varepsilon, \varepsilon_0)$, derived from eqs. (25) and (26), for quasiparticles with a mass m^* and molar volume V is given by

$$n'_F(\varepsilon, \varepsilon_0) = n_F(\varepsilon - \varepsilon_0)\left(1 + \frac{\varepsilon - \varepsilon_0}{k_B T_g}\right) \quad \text{for } \varepsilon \geqslant \varepsilon_0$$

and

$$n'_F(\varepsilon, \varepsilon_0) = 0 \quad \text{for } \varepsilon < \varepsilon_0, \tag{27}$$

with

$$n_F(\varepsilon) = \frac{V}{2\pi^2}\left(\frac{2m^*}{\hbar^2}\right)^{3/2} \varepsilon^{1/2}. \tag{28}$$

We introduced a characteristic temperature T_g defined by

$$T_g(x) = \frac{-\hbar^2}{5\gamma m^* k_B}, \tag{29}$$

where k_B is Boltzmann's constant. The value of T_F is weakly concentration-dependent due to its dependence on m^*. Typically, it is of the order of 10 K. Furthermore, we introduce a parameter g given by

$$g(x) = -T_F / T_g. \tag{30}$$

In this discussion T_F is the Fermi temperature of the ideal Fermi gas given by

$$T_F(x) = \frac{\hbar^2}{2m^* k_B}\left(3\pi^2 \frac{N_A}{V}\right)^{2/3}. \tag{31}$$

Here N_A is Avogadro's number. The value of T_g for a 1% mixture is about 100 mK and varies approximately as $x^{2/3}$. Typically, $g \approx -0.01$.

The parameter g can be rewritten as

$$g = \tfrac{5}{2}\gamma\left(\frac{3\pi^2 N_A}{V}\right)^{2/3} \tag{32}$$

which shows that g is related to the ratio of γ and square of the average particle distance.

The chemical potential is determined by

$$N_A = \int_0^\infty \frac{n'_F(\varepsilon, 0)}{1+\exp(\beta\varepsilon - \eta'_F)} d\varepsilon. \tag{33}$$

Here $\beta = 1/k_B T$ and η'_F is the reduced chemical potential, defined by

$$\eta'_F = (\mu'_F - U_0)/RT, \tag{34}$$

where R is the molar gas constant, μ'_F the chemical potential per mole of ^{3}He and $U_0 = N_A \varepsilon_0$. Introducing the Fermi functions $F_n(\eta)$ $(n > -1)$ defined by

$$F_n(\eta) = \int_0^\infty \frac{x^n}{1+\exp(x-\eta)} dx, \tag{35}$$

we obtain from eq. (33)

$$1 = \tfrac{3}{2} t^{3/2} [F_{1/2}(\eta'_F) - gt F_{3/2}(\eta'_F)]. \tag{36}$$

The parameter t represents the reduced temperature defined by

$$t = T/T_F. \tag{37}$$

The reduced chemical potential η_F of the ideal Fermi gas is determined by eq. (36) with $g = 0$:

$$1 = \tfrac{3}{2} t^{3/2} F_{1/2}(\eta_F). \tag{38}$$

In eq. (36) the argument η'_F of the function $F_{3/2}$ may be replaced by η_F as we are interested only in a first-order approximation in g. With eqs. (36), (38) and using the general relationship

$$dF_n/d\eta = nF_{n-1} \tag{39}$$

between Fermi functions, we get

$$\eta'_F = \eta_F + 2gt \left(\frac{F_{3/2}}{F_{-1/2}} \right)_F, \tag{40}$$

so for $n > 0$ to first order in g

$$F_n(\eta'_F) = \left(F_n + 2gt n F_{n-1} \frac{F_{3/2}}{F_{-1/2}} \right)_F. \tag{41}$$

The lower index F of the brackets in eqs. (40) and (41) indicates that the argument of the Fermi functions is η_F instead of η'_F. As can be deduced from eq. (38) η_F is a function of t only.

The product $gt = -T/T_g$ is equal to five times the parameter G as introduced by Bowley (1985). It plays an important role in the discussion to follow.

In low-concentration specific heat measurements gt is typically in the range -0.001 to -0.1.

The internal energy per mole of quasiparticles is given by

$$U'_F = \int_0^\infty \frac{\varepsilon n'_F(\varepsilon, 0)}{1+\exp(\beta\varepsilon - \eta'_F)} d\varepsilon. \tag{42}$$

With the density of states given by eq. (27) and using eqs. (30), (31) and (37)

$$U'_F(t, x) = U_0 + \tfrac{3}{2} R T_F t^{5/2} [F_{3/2}(\eta'_F) - gt F_{5/2}(\eta'_F)]. \tag{43}$$

The pressure satisfies

$$p'_F V = k_B T \int_0^\infty n'_F(\varepsilon, 0) \ln[1+\exp(\eta'_F - \beta\varepsilon)]\, d\varepsilon. \tag{44}$$

Integration by parts results in

$$p'_F V = R T_F t^{5/2} [F_{3/2}(\eta'_F) - \tfrac{3}{5} gt F_{5/2}(\eta'_F)]. \tag{45}$$

With eqs. (34) and (40) the chemical potential $\mu'_F = G'_F$ can be calculated. Using the general relation $G = U + pV - TS$ and using eqs. (34)–(45), the thermodynamic functions of state can be calculated. The expressions for the ideal gas can be obtained by putting $g = 0$ (and, hence $\eta'_F = \eta_F$) in these equations. The deviations of the expressions for the nearly ideal gas and the ideal gas are to first order proportional to g, and are tabulated in table 1.

2.4. *The thermodynamic properties below 250 mK*

In 1967 Radebaugh published calculations of the thermodynamic quantities of ^{3}He–^{4}He mixtures. However, his results did not agree with later measurements on the osmotic pressure (Landau et al. 1970, Ghozlan and Varoquaux 1979) and the osmotic enthalpy (de Waele et al. 1983).

Near $T = 0$ it holds that $\eta_F \simeq 1/t$. With this result the 0 K values of the thermodynamic functions of state discussed in the previous section can be calculated (table 1).

Kuerten et al. (1985) performed calculations, starting from experimental values of the molar volumes, specific heat, and the osmotic pressure at 0 K. For fixed concentrations the expressions for the ideal Fermi gas were used. The calculations were restricted to zero pressure, ^{3}He concentrations below 8%, and temperatures below 250 mK. The important features of this calculation are summarized below.

The calculation scheme is shown in fig. 1. The quantities on the top line were deduced from experiments. The molar volume V_m is given by eq. (9), where $V_4^0 = 27.58 \times 10^{-6}$ m^3/mol and $\alpha = 0.286$. The values of Π_0, the osmotic

TABLE 1

Summary of the deviations of the ideal Fermi gas behaviour, giving the general expressions, the $T=0$ and the high-temperature limits, respectively. Note the definition of the symbol $\mathscr{U}$ which is used to give an expression for the specific heat. The expression for $(\rho_{n3}V-M^*)/gM^*$ is obtained from eq. (68).

Function	Expression	Zero-T Value	High-T Value
$\frac{\mu'_F-\mu_F}{gRT_F}$	$2t^2\left[\frac{F_{3/2}}{F_{-1/2}}\right]_F$	$\frac{2}{5}$	$\frac{3}{2}t^2$
$\frac{U'_F-U_F}{gRT_F}=\mathscr{U}$	$t^2\left[\frac{3F_{3/2}}{F_{-1/2}}-\frac{F_{5/2}}{F_{1/2}}\right]_F$	$\frac{6}{35}$	$-\frac{3}{2}t^2$
$\frac{(p'_F-p_F)V}{gRT_F}$	$t^2\left[\frac{2F_{3/2}}{F_{-1/2}}-\frac{2F_{5/2}}{5F_{1/2}}\right]_F$	$\frac{8}{35}$	$\frac{3}{4}\left[\frac{t}{2\pi}\right]^{1/2}$
$\frac{S'_F-S_F}{gR}$	$t\left[\frac{3F_{3/2}}{F_{-1/2}}-\frac{7F_{5/2}}{5F_{1/2}}\right]_F$	0	$-3t$
$\frac{F'_F-F_F}{gRT_F}$	$t^2\left[\frac{2F_{5/2}}{5F_{1/2}}\right]_F$	$\frac{6}{35}$	$\frac{3}{2}t^2$
$\frac{C'_F-C_F}{gR}$	$\mathrm{d}\mathscr{U}/\mathrm{d}t$	0	$-3t$
$\frac{\rho_{n3}V-M^*}{gM^*}$	$-\frac{4}{3}t\left[\frac{F_{3/2}}{F_{1/2}}\right]_F$	$-\frac{4}{5}$	$-2t$

pressure at 0 K, were derived from measurements by Landau et al. (1970), Landau and Rosenbaum (1973) and by Ghozlan and Varoquaux (1979). The fit to a theoretical formula of Varoquaux (1971) of Landau's results for $T=0$, yields

$$\Pi_0(x)=309.2\left(\frac{x}{1+\alpha x}\right)^{5/3}-132\left(\frac{x}{1+\alpha x}\right)^{2}-691\left(\frac{x}{1+\alpha x}\right)^{8/3}\ \text{(kPa)}. \tag{46}$$

This formula was used for concentrations up to 8%.

The specific heats of pure ^{4}He and ^{3}He used in the calculations were deduced from the measurements of Greywall (1978a, b, 1982). Furthermore, a concentration-independent effective mass $m^*=2.46m_3$ was used, where m_3 is

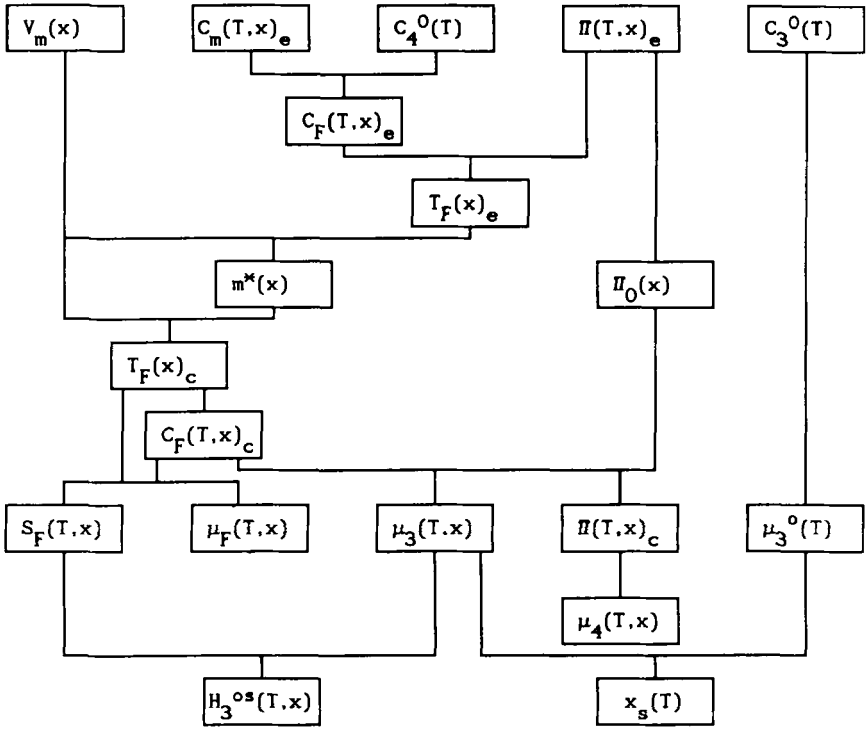

Fig. 1. Calculation scheme used by Kuerten et al. (1985) to calculate the thermodynamic functions of state below 250 mK. The quantities on the top line are the input data. The subscript e in this figure refers to quantities deduced from experiments. The subscript c refers to calculated quantities.

the ^{3}He atomic mass. As stated before, in general, m^* is concentration-dependent. However, the value of $2.46m_3$ is a good compromise between the values deduced from specific heat (Anderson 1966, Greywall 1979) and osmotic pressure for concentrations between 1% and 6.6%. Furthermore, the value is in agreement with the recent measurements of Fukuyama et al. (1988).

In a saturated solution the chemical potentials of the ^{3}He component in the concentrated phase and the dilute phase are equal. At low temperatures the ^{4}He in the concentrated phase can be neglected. The concentration of the saturated dilute solution $x_s(T)$ then follows from

$$\mu_3(T, x_s(T)) = \mu_3^0(T). \tag{47}$$

Different measurements of x_0 do not give the same result (Watson et al. 1969). The value $x_0 = 0.066$, as chosen by Kuerten, is consistent with the

measurements of Abraham et al. (1969) and Fukuyama et al. (1988). The effects of temperature and magnetization on the maximum solubility were recently discussed by Dalfovo and Stringari (1988).

The thermodynamic quantities, calculated according to this scheme, are tabulated by Kuerten et al. (1985b) as functions of x and T. The calculated osmotic pressure at finite temperatures fits Landau's data within 1%. The main results are summarized in fig. 2, which is a T^2–x diagram with lines of constant osmotic pressure (isotones), constant osmotic enthalpy and the phase separation curve. It has the same meaning and importance for dilution refrigeration as enthalpy diagrams for refrigerator engineering in general. Heat flows and cooling powers can be derived from it.

The change in (osmotic) enthalpy along the phase separation line determines the cooling power of the mixing chamber. The variation of H_3^{os} along a line of constant osmotic pressure gives the cooling power of the dilute flow in the heat exchangers in the limit of zero dissipation. Furthermore, with the isenthalps, the x–T dependence in channels with adiabatic flow of ^{3}He in ^{4}He can be determined from the temperature and concentration at the tube entrance.

The relationship between T^2 and x of the isenthalps is in good approximation linear in a large region of the T^2–x diagram as shown by the calculated diagram (fig. 2) and the measurements (see fig. 6).

The low-temperature limits of some important quantities are given in table 2. The Fermi gas entropy is

$$S_F = C_d T, \quad \text{with} \quad C_d = 104.3\ \mathrm{J\,mol^{-1}\,K^{-2}}, \tag{48}$$

and V_{m_3} the volume per mole of ^{3}He at concentration x_0 satisfies

$$V_{m_3} = 4.26 \times 10^{-4}\ \mathrm{m^3/mol}. \tag{49}$$

The validity of the calculations of Kuerten et al. was demonstrated by comparing the values of H^E at 0 K, and μ_3 determined by Seligmann et al. (1969), with the calculations.

2.5. *High-temperature limits*

Many measurements of the specific heat and the velocity of second sound are performed in the concentration and temperature region where $t \gg 1$ but still $|gt| \ll 1$. In this region one may apply the general relations given above in the high-temperature limit.

Expressions for the thermodynamic functions of the ideal Fermi gas in the high-temperature limit are given by Greywall (1979). However, our equations differ in several ways from the starting equations of Greywall (see sect. 2.3.).

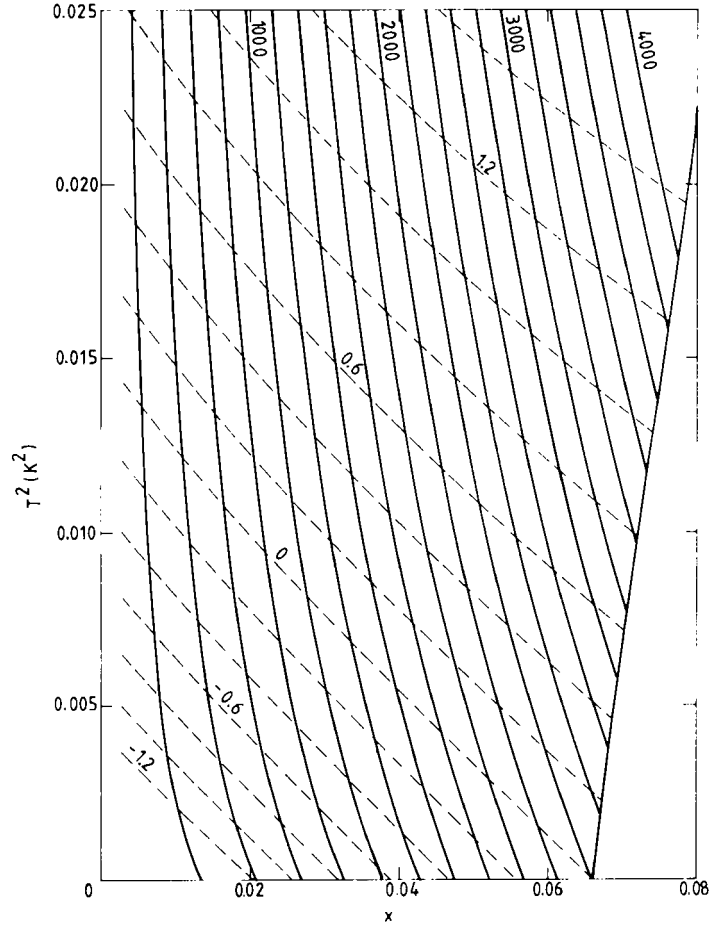

Fig. 2. The T^2–x diagram with isenthalps (dashed curves), isotones (full) and the phase separation curve, Π in Pa and H_3^{os} in J/mol.

In the high-temperature limit the Fermi functions [eq. (35)] satisfy the relation

$$F_n = nF_{n-1}, \tag{50}$$

so eq. (40) gives

$$\eta'_F \simeq \eta_F + \tfrac{3}{2}gt. \tag{51}$$

The quasiparticle internal energy is given by

$$U'_F(t, x) \simeq U_0 + \tfrac{3}{2}RT_F t(1 + Bt^{-3/2} - gt), \tag{52}$$

TABLE 2

Values of $F(0, x_0)$, F_x, F_T and F_s, where F represents x, H_3^{os}, Π, μ and μ_3, respectively. The parameters F_x and F_T represent the coefficients in the series expansion of $F(T, x)$ in the neighbourhood of $T=0$ and $x=x_0$, so $F(T, x)=F(0, x_0)+F_x(x-x_0)+F_T T^2$. The parameter F_s represents the coefficient in the series expansion along the phase separation line: $F(T, x_s)=F(0, x_0)+F_s T^2$.

F	$F(0, x_0)$	F_x	F_T	F_s
x	0.066	1	0	0.506/K^2
H_3^{os}	0 J/mol	17.58 J/mol	84.06 J/mol K^2	92.95 J/mol K^2
Π	2209 Pa	45.0 kPa	81.7 kPa/K^2	104.4 kPa/K^2
μ_3	0 J/mol	17.58 J/mol	−20.28 J/mol K^2	−11.39 J/mol K^2
μ_4	−60.92 mJ/mol	−1.242 J/mol	−2.253 J/mol K^2	−2.882 J/mol K^2

where $B=1/\sqrt{18\pi}$ gives the first-order term in the high-temperature expansion of the internal energy of the ideal Fermi gas (Stoner 1938). The high-temperature limits of the deviation of the ideal-gas functions of state are given in table 1.

The temperature derivative of eq. (52) gives C'_F:

$$C'_F \simeq \tfrac{3}{2}R(1-\tfrac{1}{2}Bt^{-3/2}-2gt)=\tfrac{3}{2}R\left(1-\tfrac{1}{2}Bt^{-3/2}+\frac{2T}{T_g}\right). \tag{53}$$

This equation shows that in the high-temperature limit the specific heat increases with temperature (de Bruyn-Ouboter et al. 1960, Greywall 1979, van der Zeeuw et al. 1984, Owers-Bradley 1988). The slope is a direct measure of T_g and, hence, of γ (Greywall 1978a, b).

Using the value of the correction of the pressure of the nearly ideal Fermi gas in the high-temperature limit (table 1) and the relation $p_F V=\frac{2}{3}U_F$ we obtain

$$p'_F=\frac{RT}{V}(1+Bt^{-3/2}+\tfrac{9}{4}Bgt^{-1/2}). \tag{54}$$

For $t \gg 1$ this equation gives van't Hoff's relation. Ebner (1967) has derived an expression for the osmotic pressure in the high-temperature limit, extending the work of Bardeen et al. (1966, 1967) to higher temperatures.

2.6. *The velocity of second sound*

The velocity of second sound is one of the main sources of information on the Fermi gas parameters of ^{3}He (van der Boog et al. 1978, 1981a, b, Greywall

1979, Greywall and Paalanen 1981, Husson et al. 1983, Corrucini 1984, Bowley 1985, 1988). The basic equations for the velocities of first sound, u_+, and second sound, u_-, are given by Khalatnikov (1965):

$$2u_\pm^2 = (1+d)u_2^2 + u_1^2 \pm \{[(1+d)u_2^2 + u_1^2]^2 - 4u_1^2u_2^2\}^{1/2} \tag{55}$$

where the plus sign holds for first sound and the minus sign, for second sound. In eq. (55) u_1 is given by

$$u_1^2 = (1+d)\left(\frac{\partial p}{\partial \rho}\right)_T, \tag{56}$$

and u_2,

$$u_2^2 = \frac{M_m}{M_4^2}\frac{\rho_s}{\rho_n}\frac{w}{1+d}, \tag{57}$$

where

$$w = S_4^2\left(\frac{\partial T}{\partial S_m}\right)_x - x\left(\frac{\partial \mu_4}{\partial x}\right)_T \tag{58}$$

and

$$d = \frac{M_m^2}{M_4^2}\frac{\rho_s}{\rho_n}\left(\frac{x}{\rho}\left(\frac{\partial \rho}{\partial x}\right)_T\right)^2, \tag{59}$$

where S_4 is the partial entropy of the ^{4}He component and u_2 is equal to the velocity of second sound to first-order. In these expressions M_m is the molar mass of the mixture, M_4 is the ^{4}He molar mass, ρ_s (ρ_n) is the superfluid (normal fluid) density and ρ is the density of the solution.

The relative difference of u_-^2 and u_2^2 is about $(u_2/u_1)^2 d$. The ratio u_2/u_1 is typically 0.1, and $d \approx 0.16x$. Therefore, practically speaking, $u_- \approx u_2$.

From eq. (57), ρ_n can be derived from the measured velocity of second sound, provided the temperature and concentration dependences of w and d are known. The so-called "inertial effective mass" can be obtained from this by subtracting the density of the normal ^{4}He–II component.

In this section we discuss the relations for the velocity of second sound within the framework of the previous sections. A theory of first and second sound has been given by Brucker et al. (1976).

Equation (58) can be simplified as follows. $S_4 = -(\partial \mu_4/\partial T)_x$, so $S_4(\partial T/\partial S_m)_x = -(\partial \mu_4/\partial S_m)_T$. Hence,

$$w = -S_4\left(\frac{\partial \mu_4}{\partial S_m}\right)_x - x\left(\frac{\partial \mu_4}{\partial x}\right)_T. \tag{60}$$

With

$$\left(\frac{\partial \mu_4}{\partial x}\right)_T = \left(\frac{\partial \mu_4}{\partial x}\right)_{S_m/x} + \left(\frac{\partial \mu_4}{\partial S_m/x}\right)_x \left(\frac{\partial S_m/x}{\partial x}\right)_T \tag{61}$$

and eq. (4) we obtain

$$w = -x\left(\frac{\partial \mu_4}{\partial x}\right)_{S_m/x}. \tag{62}$$

This expression for w has been derived before by Ghozlan and Varoquaux (1969). Together with eq. (17) it shows very elegantly that second sound can be considered as an adiabatic osmotic pressure wave (Corrucini 1984). Note that eq. (62) does not contain the parameter α as erroneously derived by Bowley (1985).

We will consider the expression for the second-sound velocity in the temperature region where the ^{4}He contribution to the entropy can be neglected (so $S_m/x = S'_F$), and at the same time the high-temperature limiting values of the Fermi gas properties can be applied. In this case the contribution of the pure ^{4}He chemical potential (the fountain term) may be neglected and we may write

$$\left(\frac{\partial \mu_4}{\partial x}\right)_{S'_F} = -V_4^0\left(\frac{\partial p'_F}{\partial x}\right)_{S'_F}. \tag{63}$$

In order to obtain the high-temperature limit we write

$$\left(\frac{\partial p'_F}{\partial x}\right)_{S'_F} = \left(\frac{\partial p'_F}{\partial x}\right)_t + \left(\frac{\partial p'_F}{\partial t}\right)_x \left(\frac{\partial t}{\partial x}\right)_{S'_F}. \tag{64}$$

We use eq. (54) and note that $(\partial t/\partial x)_{S_F}$, is, to first order, proportional to g. Therefore, we may put $p'_F = p_F$ in the second term, as the difference between p'_F and p_F results only in a term which is of second order in g. After a little algebra, expressing the first term in α and δ (de Waele and Kuerten 1989), we obtain

$$w = \tfrac{5}{3}xRT(1 + Bt^{-3/2} - 2\alpha x - \tfrac{3}{5}\delta x + \tfrac{4}{5}gt), \tag{65}$$

where eqs. (9), (13), (31) and (32) are used. The parameter δ determines the concentration dependence of the effective mass according to

$$m^*(x) = m_0^*(1 + x\delta), \tag{66}$$

where m_0^* is the quasiparticle effective mass at zero concentration.

Expression (57) contains the normal fluid density ρ_n which also contains a contribution from the ^{3}He component. This contribution is given by Wilks (1967) and Greywall (1979):

$$\rho_{n3} = -\tfrac{1}{3}\frac{\hbar^2}{\pi^2}\int_0^\infty \frac{\partial f_{FD}}{\partial \varepsilon} k^4 \, dk, \tag{67}$$

where $f_{FD}=[1+\exp\{\beta(\varepsilon-\varepsilon_0)-\eta'_F\}]^{-1}$. After integration by parts, ρ_{n3} can be expressed in terms of Fermi functions according to

$$\rho_{n3}=\frac{M^*}{V}\left[1-\tfrac{4}{3}gt\frac{F_{3/2}}{F_{1/2}}\right]_F \tag{68}$$

with $M^*=m^*N_A$.

Using the high-temperature limiting values of the Fermi functions with eqs. (9) and (66) gives to first order in αx, δx and g

$$\rho_{n3}=x\frac{M_0^*}{V_4^0}(1-\alpha x+\delta x-2gt). \tag{69}$$

Furthermore,

$$\rho_s\simeq\rho-\rho_{n3}\simeq\frac{M_4}{V_4^0}\left[1-0.25x-\alpha x-x\frac{M_0^*}{M_4}\right] \tag{70}$$

and

$$\frac{M_m}{M_4}=1+\frac{M_3-M_4}{M_4}x=1-0.25x. \tag{71}$$

Finally, we note that the parameter d [eq. (59)] is to lowest order given by

$$d\simeq x\frac{M_4}{M_0^*}\left[\frac{M_3-M_4}{M_4}-\alpha\right]^2=\frac{M_4}{M_0^*}(\alpha+0.25)^2x. \tag{72}$$

Combining the equations given above results in the equation

$$u_2^2\simeq\frac{5RT}{3M_0^*}\left[1+Bt^{-3/2}+2.8gt-1.6\delta x-2\alpha x-d-0.5x-\frac{M_0^*}{M_4}x\right]. \tag{73}$$

Equation (73) contains terms due to the Fermi character of the quasiparticles ($Bt^{-3/2}$), the deviation of the ideal gas excitation spectrum ($2.8gt$), the concentration dependence of the effective mass ($-1.6\delta x$), and the concentration dependence of the molar volume (the α-dependent terms), respectively. It clearly shows the relative importance of each of the contributions.

The data of Greywall (1979), and Greywall and Paalanen (1981) have been reanalyzed by Bowley (1985, 1988).

2.7. *Summary of experimental results*

The first experimental data on mixture properties at low temperatures were analyzed in terms of the ideal Fermi gas. After the discovery of the non-parabolic excitation spectrum the data have been analyzed according to this new insight. This was encouraged by the availability of high-precision data

on the specific heat and the velocity of second sound. Bowley (1985) fitted the data of Greywall (1979), and Greywall and Paalanen (1981) taking into account the effects of the interactions between the ^{3}He quasiparticles and their dispersion. Recently, the same data were reanalyzed once more (Bowley 1988) using the new temperature scale introduced by Greywall (1985). The value of the parameter γ is found to be about -0.08 Å^2.

Heat capacity measurements of 0.44%, 1.07% and 2.6% mixtures, were performed by Owers-Bradley et al. (1987). In this paper they also gave a short review of the various experimental results of the quasiparticle effective mass at zero concentration. For completeness we present a summary in table 3.

3. Hydrodynamics: experimental results

3.1. *Introduction*

In the early days of dilution refrigeration the possible existence of mutual friction between ^{3}He and ^{4}He was a source of concern. The first ^{3}He circulating machine (Das et al. 1964) was equipped with a superleak shunt in the dilute channel to avoid possible harmful effects of mutual friction. Wheatley and his co-workers (1968b, 1971) designed ^{3}He circulating dilution refrigerators taking only viscous effects and heat conduction into account. In 1971, they measured the temperature increase in a flow impedance consisting of an annular space between two cylinders. The results were in agreement with the so-called mechanical-vacuum model. This is a model in which the

TABLE 3
Summary of the experimental values of m_0^*.

References	m_0^*/m_3	Method
Edwards et al. (1965)	2.5	Specific heat
Anderson et al. (1966)/Landau et al. (1970)	2.34	Specific heat
Landau et al. (1970)	2.24	Osmotic pressure
Varoquaux (1971)	2.26	Osmotic pressure
Greywall (1978a, b)	2.28	Specific heat
Greywall (1979)	2.341	Specific heat, Second sound
Sobolev et al. (1979)	2.28	Normal component density
Ghozlan and Varoquaux (1979)	2.255	Review
Polturak and Rosenbaum (1981)	2.38	Specific heat
Chocolacs et al. (1984)	2.34	Specific heat
Owers-Bradley et al. (1987, 1988)	2.226	Specific heat
Bowley (1985, 1988)	2.272	Second sound

^{3}He is assumed to move with respect to the superfluid ^{4}He without mutual friction. Possibly, as a result of the successful operation of machines without superleak the question of the existence of mutual friction in mixtures was shifted to the background.

Discrepancies with the mechanical-vacuum model have been reported occasionally, especially, in high-circulation machines. In 1971, Niinikoski reported the observation of large osmotic pressure differences between the mixing chamber and the still, which were not compensated by a fountain pressure or by a pressure drop due to the viscosity of the solution. In 1977, anomalous dependence of the ^{3}He flow rate as a function of the still heating power was observed in Grenoble (Frossati et al. 1977).

At the Eindhoven University of Technology, a more extensive study on these discrepancies was triggered by the discovery of the anomalous behaviour of the difference in heights of the phase boundaries in a double mixing chamber (Coops et al. 1982).

In this section, firstly, experimental work concerning the flow properties above 0.7 K are discussed. In the main part of this section, the results of the investigations in Eindhoven, concerning the flow properties below 250 mK, are described.

3.2. *Flow properties in the 0.7–2.17 K range*

At temperatures above 0.7 K the ^{3}He flow properties are dominated by the strong coupling with the normal ^{4}He component. This leads to the so-called "heat flush" effect where a heat flow in a ^{3}He–^{4}He mixture carries the ^{3}He along with the normal component of the ^{4}He. In experiments where the ^{3}He is not circulated, it is very difficult to obtain a stationary state. In principle, ^{3}He can be circulated as in a ^{3}He dilution refrigerator but, to our knowledge, this kind of experiments has never been performed at high temperatures.

In the early days of the mixture investigations, the heat-flush effect was used to increase the ^{3}He concentration starting from natural helium. In Lancaster, McClintock and his co-workers developed a technique based on the heat-flush effect to purify natural helium to an extremely high degree ($x < 5 \times 10^{-13}$) (Hendry and McClintock 1987). With high-purity ^{4}He it is now possible to study advanced topics such as the determination of the Landau critical velocity (Ellis and McClintock 1985), and macroscopic quantum tunneling of vortices in He-II (Hendry et al. 1988).

In Leiden, Mudde and van Beelen (1987), and Mudde (1989) have investigated thermal counterflow properties of mixtures in a capillary of inner diameter $D = 0.1$ mm (fig. 3) above 1 K. Below normal-component velocities of $v_c = 106$ mm/s the temperature along the tube was remarkably constant. This is the result of the requirement that in quasisteady flow the entropy flow

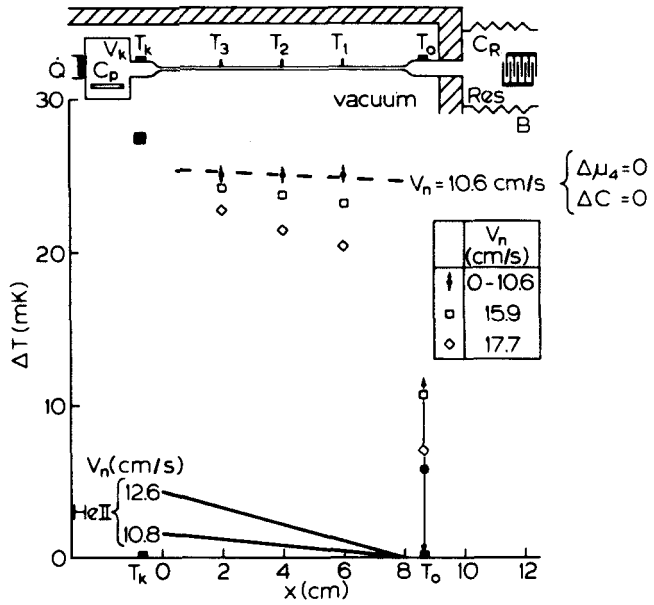

Fig. 3. Experimental set-up and results from the Leiden group (Mudde and van Beelen 1987). The top of the figure represents the experimental arrangement. A heating power $\dot{Q}$ is supplied to cell V_k containing a ^{3}He–^{4}He mixture. The pressure in the cell is measured with a pressure gauge C_p. The cell is connected with a reservoir via a capillary of inner diameter 0.1 mm. The temperature profile is measured with five thermometers. The time variation of the concentration in the reservoir is measured with a parallel-plate capacitor. In the lower part of the figure the points represent the temperatures in a quasisteady flow experiment, measured at the moment when $T_k - T_0$ passes the (arbitrary) value of 27.5 mK. All temperature profiles for normal fluid velocities below 106 mm/s coincide, and the T-gradient is zero. For velocities larger than this value the temperature gradient is nonzero and flow-dependent.

and the ^{3}He flow must be almost constant. The product $v_c D = 10.6$ mm^2/s is in agreement with the corresponding product in pure ^{4}He-II (see, e.g. Tough 1982) and in ^{3}He–^{4}He mixtures below 250 mK (Zeegers et al. 1987).

Partly as a result of their work on the vortex cooler, Satoh and his co-workers (Okuyama et al. 1987) in Sendai have studied the flow properties in the 0.7–1.3 K range. NMR was used to measure the time dependence of the ^{3}He concentration in an upstream cell, from which the normal-component velocity is derived. The measurements in 0.1 and 0.2 mm diameter tubes showed two critical velocities with $v_c D$ products of 25 and 50 mm^2/s, respectively. These values are about a factor 2 higher than those found by other authors.

We like to point out that the temperature region of 0.5 to 1.2 K is very interesting since here the transition takes place from the low-temperature

regime, where the phonons and rotons can be completely neglected, to the high-temperature regime where the flow is dominated by these ^{4}He excitations. Unfortunately, so far, no systematic investigations have taken place in this temperature region.

3.3. *Flow properties in the 10–250 mK range*

3.3.1. *Introduction*

Below 500 mK the densities of the phonons and the rotons are low and have a negligible effect on the ^{3}He flow properties. In this temperature region, steady-state experiments are fairly easy to perform. The ^{3}He-circulating dilution refrigerator is the natural instrument for studying the ^{3}He–^{4}He flow properties. For an introduction to dilution refrigeration we refer to the book of Lounasmaa (1974).

In this section we describe the experiments at temperatures between 10 and 250 mK, performed at the Low Temperature Physics group of the Eindhoven University of Technology (see Castelijns et al. 1985, Kuerten et al. 1986a, b). In these experiments the changes of the pressure, temperature and ^{3}He concentration across a large variety of flow impedances were determined. Three flow rate regimes can be distinguished: the high flow rate regime, where the gradient of the ^{4}He chemical potential in a cylindrical capillary satisfies a cubic velocity dependence; a low flow rate regime, where μ_4 is constant; and a transition region, where critical velocities are observed.

Here we first give the experimental set-up. Next, the experimental results in the high flow rate regime are described. Finally, the measurements of the critical velocities are presented.

3.3.2. *Experimental set-up*

The total molar rate of circulation in a dilution refrigerator, $\dot{n}_t$, is the sum of the ^{3}He circulation rate $\dot{n}_3$ and the ^{4}He circulation rate $\dot{n}_4$. It is imposed by the heating power $\dot{Q}_s$ supplied to the still. The ^{4}He flow rate $\dot{n}_4$ is, typically, a few percent of $\dot{n}_t$ and will be neglected.

The mixing chamber (M) has an experimental cell (E) on top (fig. 4). In this context, lower indices m or e apply to properties in M or E, respectively.

The temperature T_m of the mixing chamber is imposed by means of a heater on the entrance tube. The ^{3}He enters the mixing chamber at temperature T_i. It leaves the mixing chamber in the dilute phase through the flow impedance Z_m and flows into the experimental cell E. The exit of E is connected to the dilute side of the heat exchangers. In E the temperature T_e and the ^{3}He concentration x_e are measured.

The flow impedance Z_m is the flow channel under investigation. In general, it consists of a cylindrical capillary of length L and inner diameter D with

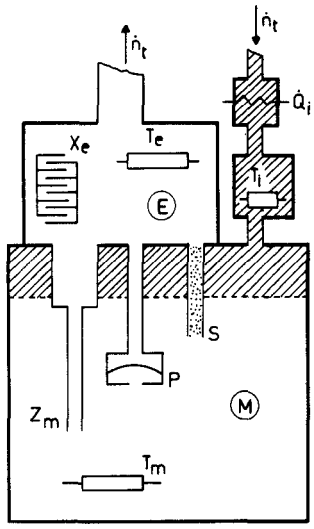

Fig. 4. Experimental set-up of the Eindhoven group. The mixing chamber (M) and an experimental cell (E) are connected by a flow impedance Z_m. The temperatures at the mixing chamber entrance (T_i), in the mixing chamber (T_m), and in the experimental cell (T_e) are measured. The ^{3}He concentration in E is measured with a plate capacitor. The pressure drop across the impedance is measured by a pressure gauge. In some cases the flow impedance was shunted by a superleak. The temperature T_m is kept constant by adjusting the heating power $\dot{Q}_i$ at the entrance of the mixing chamber.

$L \gg D$. Tubes with lengths varying from 5 mm to 1.4 m and diameters from 0.1 to 2.3 mm are investigated. Also, bundles of (sometimes more than 100) parallel capillaries, and slits are studied.

Optionally, a superleak can be installed parallel to the flow impedance permitting ^{4}He to circulate through Z_m and the superleak (Castelijns et al. 1985). In this review only experiments without superleak shunt will be discussed. In nonadiabatic flow experiments a heating power is supplied to the liquid flowing in Z_m. Here we will concentrate on results of adiabatic flow experiments.

The ^{3}He concentration of the mixture in E is measured with an air capacitor using the fact that the relative dielectric constant ε_r of ^{3}He–^{4}He mixtures is equal to $1.0572-0.0166x$ (Kierstead 1976). The capacitor consists of 23 plates with a clear distance of 0.2 mm (nominal capacitance 32 pF). The capacitance is measured with a bridge. The calibration is obtained from the values of the capacitance in vacuum, in pure ^{4}He, and in the saturated mixture (6.6%).

The ^{3}He concentration in the mixing chamber, x_m, is calculated from the measured temperature T_m and the relation for the phase separation line (Kuerten et al. 1985b).

The pressure drop Δp in the impedance is measured with a pressure gauge. In this gauge the capacitive coupling between a silver-plated Kapton foil and a fixed surface is a measure of the pressure difference across the foil. The gauge was calibrated in a ^{4}He cryostat against the hydrostatic pressure head of a ^{4}He liquid column for pressures between 0 and 300 Pa.

The values of the osmotic pressures and chemical potentials of the mixtures in E and M are derived from the measured temperatures and concentrations using the expressions given by Kuerten et al. (1985a, b). The osmotic pressure in the still is measured with a so-called London device (London et al. 1968, Varoquaux 1971).

3.3.3. *Experimental results, the high flow rate regime*

When the flow rate is increased at fixed T_m, the ^{3}He concentration x_e decreases. The concentration is observed to vary linearly with the distance l from the tube entrance. This holds even for concentrations varying from 6.6% at the entrance to values as low as 3% at the exit.

In fig. 5 some typical results of x_e–$\dot{n}_t$ measurements are given. The concentration at the entrance $x_m \approx 6.6\%$. For most of the tubes the concentration x_e decreases monotonically with increasing flow rate. Curve 4 represents the results of a tube with a small diameter (0.8 mm). It shows a kink at $\dot{n}_t = 0.3$ mmol/s. For $\dot{n}_t > 0.3$ mmol/s, the concentration $x_e \approx 1.3\%$. Such a low

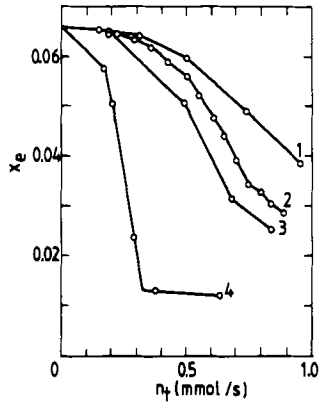

Fig. 5. Measured x_e–$\dot{n}_t$ dependencies for four different sizes of Z_m: (1) $L = 23$ mm, $D = 1.6$ mm; (2) $L = 10.5$ mm, $D = 1.2$ mm; (3) $L = 23$ mm, $D = 1.2$ mm; (4) $L = 23$ mm, $D = 0.8$ mm. The measurements are performed in the high flow rate regime, where mutual friction dominates. The lines are guides to the eye only.

x_e value causes a very low ^{3}He concentration in the liquid in the still, resulting in a high ^{4}He contribution in the circulating mixture. Increasing the still heating power results only in a larger ^{4}He contribution.

The conservation of energy for a steady adiabatic flow of ^{3}He through ^{4}He–II is formulated in eq. (23). In the T–x region of interest (10–150 mK, 2–7% ^{3}He), the enthalpy H_3^{os} is, in good approximation, a linear function of T^2 and x (fig. 2). Therefore, it is convenient to plot the experimental data in a T^2–x diagram.

In fig. 6 the measured T_e^2–x_e dependences are plotted for varying $\dot{n}_t$ and fixed T_m (by adjusting $\dot{Q}_i$ every time $\dot{n}_t$ is varied). The measured T_e^2–x_e curves follow lines of constant osmotic enthalpy. When the flow rate is increased, the temperature T_e increases and the concentration x_e decreases along an isenthalp. Eventually, at large flow rates, T_e will approach the temperature T_i of the ^{3}He entering the mixing chamber. But T_e can never be larger than T_i because the concentrated phase is cooled by the liquid in the dilute side of the heat exchangers. In practice, the upper limit for T_e is $0.9T_i$. When no heating

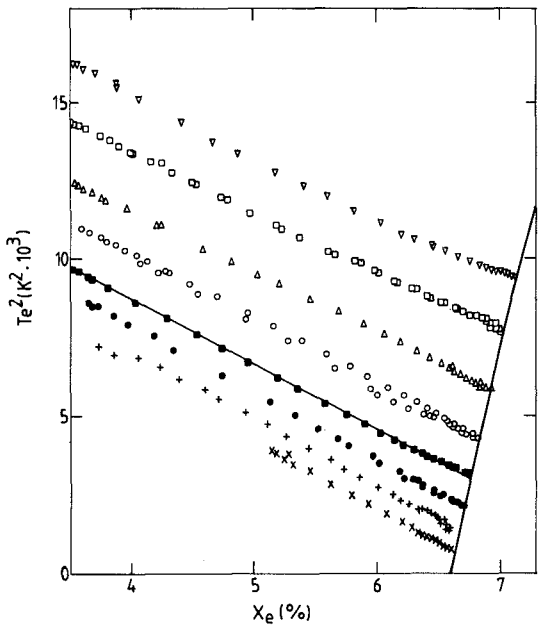

Fig. 6. T^2–x diagram. The points represent measured dependences of T_e^2 and x_e when $\dot{n}_3$ is varied at fixed T_m. Curves are shown for eight different mixing chamber temperatures. The points follow the lines of constant osmotic enthalpy in fig. 2. The line through one of the series of points represents the line of constant osmotic enthalpy in the low-temperature limit (see table 2). The heavy line represents the phase separation line.

power is applied to the mixing chamber $T_i = 2.8T_m$, so we get as the limiting case $T_e \approx 0.9T_i \approx 2.5T_m$. The limiting T_e^2–x_e relation is given by

$$T_e^2 = 0.25(x_0 - x_e)K^2. \tag{74}$$

The pressure difference Δp is measured as a function of $\dot{n}_3$ for fixed values of T_m in the range between 30 and 90 mK. From the measured T_e, x_e and Δp values, the ^{4}He chemical potential μ_{4m} is calculated. The values of x_m and μ_{4m} are obtained from the tabulated values at the coexistence curve.

In fig. 7, some examples of the cube root of $\Delta\mu_4 = \mu_{4e} - \mu_{4m}$ are plotted as functions of $\dot{n}_3$ for flow rates much larger than the critical flow rate. The measured gradient of μ_4 and the ^{3}He flow rate density $j_3 = \dot{n}_3/A$ satisfy the relation

$$\frac{d\mu_4}{dl} = \chi j_3^3, \tag{75}$$

where χ is an empirical parameter equal to 11×10^{-9} kg s m^7/mol, which is not strongly temperature- and concentration-dependent. The total area of the cross section of the impedance is A. Relation (75) is of key importance for the understanding of mutual friction. It will be discussed in more detail in the next sections.

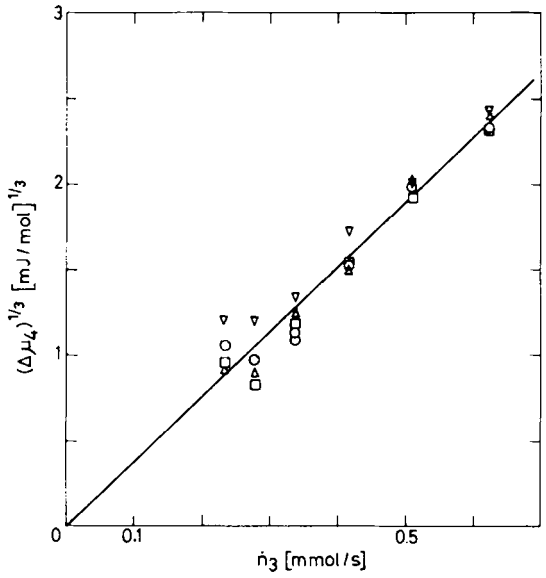

Fig. 7. The cube root of $\Delta\mu_4 = \mu_{4e} - \mu_{4m}$ as a function of $\dot{n}_3$. The symbols correspond to four different mixing chamber temperatures.

The osmotic pressures Π_s (the osmotic pressure in the still) and Π_e are equal within the uncertainties of the measurement. Large differences between Π_e and Π_m are observed even though the pressure drop for the impedance used in the experiment was very small. This is a direct result of eqs. (17) and (75) which also explain the observation of Niinikoski (1971).

The pressure drop Δp over Z_m depends on the flow rate, the sizes of Z_m, and the temperature T_m. In general, Δp is determined by the combined effect of mutual friction and viscosity. At high flow rate densities in single tubes, the measured pressure differences are very small (1 Pa). It will be shown in sect. 4.4. that in these experiments mutual friction strongly dominates viscous effects. In order to investigate the combined-dissipation regime, where both viscosity and mutual friction play an important role, impedances are constructed consisting of bundles of N identical parallel tubes each with diameter D_N and length L. The diameters D_N are chosen in such a way that the total cross-sectional area of the various impedances is approximately constant ($\frac{1}{4}N\pi D_N^2 \approx 2\ \mathrm{mm}^2$). In this way the viscous contribution is increased when N was increased, while the mutual friction term is unchanged.

In fig. 8 measured pressure differences over a bundle of 28 tubes are plotted for several values of T_m as functions of $\dot{n}_3$. At low flow rates the viscous effects dominate. The values of the constant η_d, giving the ^{3}He viscosity η, according to

$$\eta = \eta_d / T^2, \tag{76}$$

are derived from the linear part of these graphs using the relation

$$\frac{dp}{dl} = -\eta Z \dot{n}_3 V_m / x. \tag{77}$$

The η_d values vary roughly from 50 nPa s K^2 at $T_m = 30$ mK to 65 nPa s K^2 at $T_m = 60$ mK, in agreement with the measurements of Kuenhold et al. (1972). For higher flow rates the increasing temperature in the tube leads to a decreasing viscosity of the mixture. This effect results in a concave Δp–$\dot{n}_3$ relationship.

3.3.4. *Critical velocities*

In this section we describe the observation of nonzero critical velocities in ^{3}He–^{4}He mixtures in flow channels consisting of bundles of parallel tubes. As usual, the ^{3}He flow rate was varied at constant T_e.

A typical example of the measured downstream temperature T_e plotted as a function of the average ^{3}He velocity is given in fig. 9. Sóme of the measurements seem to show hysteresis around the transition. The critical velocity is not strongly temperature-dependent. This suggests that the critical

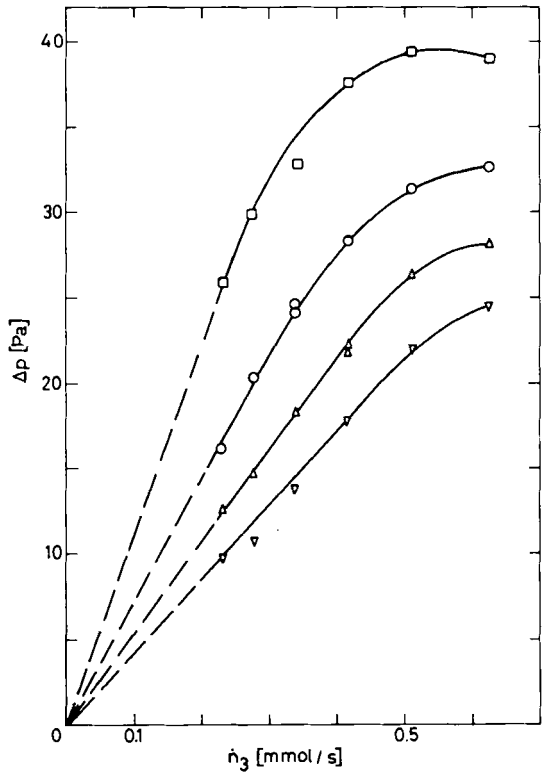

Fig. 8. Pressure differences across a bundle of 28 parallel capillaries as functions of $\dot{n}_3$ for several constant values of T_m. The lines are for visual aid only. The parameter η_d is determined from the linear part of the curves.

velocity is only a function of the density of the normal component, which does not change more than 3% in the temperature range.

The critical velocity increases with decreasing tube diameter. The product $v_c D$ is plotted as a function of the diameter in fig. 10. For diameters above 0.3 mm the value is about 15 mm^2/s, comparable with the value in pure ^{4}He–II.

Below the critical velocity $\Delta\mu_4 = 0$. Just above the critical velocity the value of $\Delta\mu_4$ is not given by eq. (75), which is the limiting value at large flow rates.

Later on, Zeegers et al. (1989) found indications of a second critical velocity v_{c2} in cylindrical capillaries. The values are about twice the first critical velocity v_{c1}. No critical velocity is observed in flow impedances consisting of

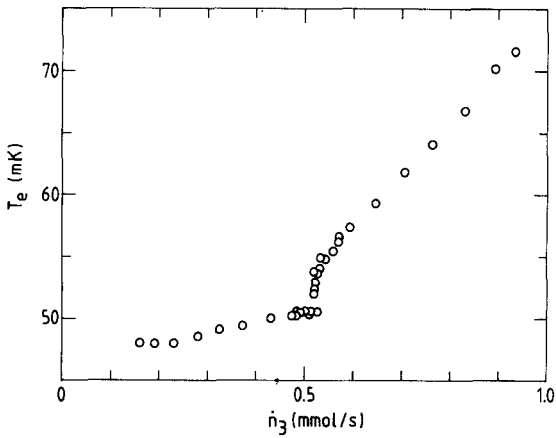

Fig. 9. The measured temperature T_e as a function of $\dot{n}_3$ for $T_m = 46$ mK, determined with a flow impedance consisting of a bundle of 60 parallel capillaries, with $L = 177$ mm and $D = 0.3$ mm. The critical velocity at a flow rate of about 0.55 mmol/s is clearly visible.

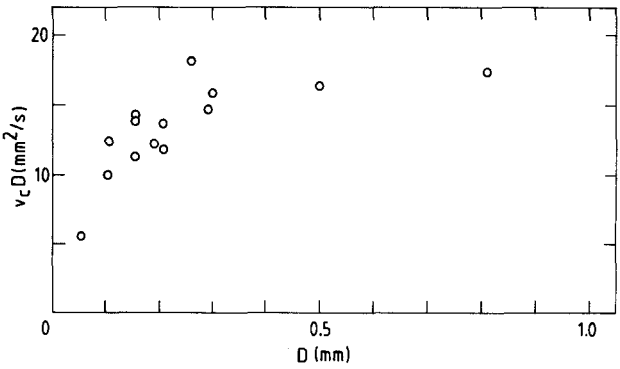

Fig. 10. The product $v_c D$ versus D.

narrow slits. Presumably, the critical velocity is very small or zero in slits. Apparently, the appearance of critical velocities is determined by the geometry of the flow channel. It is an intriguing question whether the ratio v_{c2}/v_{c1} in cylindrical capillaries is equal to 2 for a fundamental reason. Probably, this question can only be answered when the mechanism for critical velocities is understood.

At present there is no complete empirical description for the transition from the state where mutual friction is absent to the fully developed mutual-friction state. We have the impression that numerical experiments with the superfluid vortex tangle will contribute significantly to the understanding of superfluid hydrodynamics. Theoretical aspects of the ^{3}He–^{4}He hydrodynamics will be treated in the next section.

4. Hydrodynamics: theoretical aspects

4.1. *Introduction*

The hydrodynamic description of ^{3}He–^{4}He-II mixtures leans heavily on the two-fluid model of *pure* superfluid ^{4}He-II, developed by Landau in 1941 (Tough 1982, Glaberson and Donnely 1985). In this model, phonons and rotons cannot be created by the motion of the normal component below certain well-defined values of the relative velocity between the superfluid and the normal component. This is imposed by energy and momentum conservation. The critical velocity for roton excitation is the smallest, 58 m/s, and, therefore, no friction (dissipation) should occur at relative velocities below this value. For normal-component velocities below 58 m/s the superfluid background was expected to behave as a mechanical vacuum.

However, already in 1949, Gorter and Mellink showed the existence of a frictional force between the normal and the superfluid components in pure ^{4}He above velocities as low as a few centimeters per second. Onsager (1949) conjectured vortices of superfluid ^{4}He with quantized circulation as a possible third kind of excitation. Following a suggestion of Feynman (1955), Vinen (1957) developed a model in which the frictional force between the normal and the superfluid components is mediated by vortices. When a critical velocity is exceeded the vortices are assumed to form a tangle in the fluid which is in violent motion (superfluid turbulence).

The mechanical-vacuum model for ^{3}He–^{4}He mixtures has its origin in a paper by Landau and Pomeranchuk (1948). In contrast to the situation in pure ^{4}He the possibility of mutual friction in mixtures has long been overlooked. Since the work of Mazur and Prigogine (1951) mutual friction between ^{3}He and ^{4}He has not been considered. Khalatnikov (1965) derived the two-fluid hydrodynamic equations for ^{3}He–^{4}He-II mixtures neglecting mutual friction. In this section the hydrodynamics of ^{3}He–^{4}He mixtures will be treated including mutual friction. Some basic properties of quantized vortices will be treated. Finally, the differential equation for the temperature profile in a cylindrical tube in which ^{3}He flows through superfluid ^{4}He will be derived.

4.2. *Hydrodynamic equations*

The hydrodynamic equations for pure ^{4}He-II and for ^{3}He–^{4}He-II mixtures have been derived by Khalatnikov (1965) without taking mutual friction into account. If mutual friction is included, an extra term appears in the equation of motion of the superfluid component. Here we only give an outline of the tedious derivation which is given in more detail in the thesis of Kuerten (1987b).

The treatment is analogous to the one given by de Groot and Mazur (1962) for a classical multicomponent fluid. In the derivation it is assumed that the temperature is low enough to neglect the normal component of ^{4}He, apart from its effect on the effective mass. The equation of motion for the superfluid component reads

$$\frac{\partial \boldsymbol{v}_s}{\partial t}+(\boldsymbol{v}_s\cdot\nabla)\boldsymbol{v}_s+\nabla\left(\frac{\mu_4}{M_4}+h\right)=\boldsymbol{f}, \tag{78}$$

where h is a dissipative potential. The right-hand side of eq. (78) is the mutual frictional force exerted by the normal component on the superfluid component per unit mass of the superfluid component. In the derivation the equations for conservation of total mass, ^{3}He particle number, total momentum, and energy, together with the equation for the entropy production and eq. (78) provide ten equations for nine variables. From this overspecified set the dissipative function can be determined as a sum of terms, each of which is the product of a generalized thermodynamic force and a flux. For a large class of irreversible processes the relations between the fluxes and forces are linear to first order. In general, higher-order relationships are allowed, provided the dissipative function is positive. To first order the mutual frictional force would read

$$\boldsymbol{f}=-\frac{\beta}{T}\nabla T+\gamma\rho_s(\boldsymbol{v}_n-\boldsymbol{v}_s). \tag{79}$$

As shown in sect. 3.3, the mutual friction is zero below a certain critical velocity. Above the critical velocity, the relationship between $\boldsymbol{f}$ and the velocity difference is nonlinear. At high velocities the frictional force is, in good approximation, proportional to the cube of the relative velocity:

$$\boldsymbol{f}\approx B\rho_n|\boldsymbol{v}_n-\boldsymbol{v}_s|^2(\boldsymbol{v}_n-\boldsymbol{v}_s), \tag{80}$$

where B is a positive function of T and x. In writing down eq. (80) the effect of ∇T on $\boldsymbol{f}$ has been neglected. The nonlinear dependence is the result of the interaction of the normal component with the superfluid through quantized vortices as will be discussed in the next section.

4.3. *The motion of quantized vortices*

From the analogy with flow in pure ^{4}He-II it is expected that mutual friction in ^{3}He–^{4}He mixtures is due to the interaction of ^{3}He with quantized vortex lines in superfluid ^{4}He. The idea is that these vortex lines are created (or form a stable tangle) if the average relative velocity between ^{3}He and ^{4}He exceeds a certain critical value. As a result of the vortex–vortex interactions and the interaction with ^{3}He, the vortex lines develop towards a complex dynamical structure, which is called a vortex tangle.

If the force between ^{3}He and a single straight vortex line is known, the equation of motion for a vortex line can be constructed. Then one can calculate the evolution of a vortex tangle numerically, starting from an arbitrary initial configuration. In the steady-state macroscopic properties like the line length density L and the mutual frictional force density $\boldsymbol{F}$ fluctuate around an average value.

The procedure outlined above has been followed by Schwarz (1982, 1985) for pure ^{4}He, where the force between the normal component and a straight vortex line is known from experiments. Unfortunately, the force between ^{3}He and a vortex line is unknown. However, it is possible to use a general expression for this force with only two unknown friction parameters, which may be dependent on temperature and ^{3}He concentration. Then, the unknown quantities L and $\boldsymbol{F}$ can be determined as functions of these two parameters and the relative velocity.

The equation of motion of a vortex line has been derived by Schwarz (1978). Two contributions to the velocity of a point on the vortex line can be distinguished. The first contribution is due to the local superfluid velocity $\boldsymbol{v}_0$. This local velocity $\boldsymbol{v}_0$ differs from the hydrodynamic superfluid velocity $\boldsymbol{v}_s$, which equals the average of $\boldsymbol{v}_0$ over a volume containing many vortex lines. The second contribution results from the force of the normal component on the vortices. This force is transferred to the superfluid as a Magnus force. It causes a difference between the local superfluid velocity and the velocity of the vortex line, which is proportional to the velocity of the normal fluid with respect to the line. The general expression for the velocity of a vortex line, $\boldsymbol{v}$, is

$$\boldsymbol{v}=\boldsymbol{v}_0+\alpha \boldsymbol{s}'\times(\boldsymbol{v}_n-\boldsymbol{v}_0)-\alpha' \boldsymbol{s}'\times[\boldsymbol{s}'\times(\boldsymbol{v}_n-\boldsymbol{v}_0)], \tag{81}$$

where $\boldsymbol{s}'$ is the unit vector tangent to the vortex line, and α and α' are friction parameters. For a given configuration of the vortices, eq. (81) yields the time evolution if $\boldsymbol{v}_0$ is known. The local superfluid velocity obeys the relations

$$\nabla\times\boldsymbol{v}_0=0 \tag{82}$$

and

$$\oint_C \boldsymbol{v}_0\cdot \mathrm{d}\boldsymbol{l}=\kappa=h/m_4 \tag{83}$$

if the contour C is taken around one vortex line with positive orientation. When the fluid is incompressible

$$\nabla \cdot \boldsymbol{v}_0 = 0 \tag{84}$$

holds, and the relations are similar to the equations for a magnetic field due to electrical currents and give the Biot–Savart solution (see e.g. Jackson 1975)

$$\boldsymbol{v}_0(\boldsymbol{r}, t) = \boldsymbol{v}_{s0} + \frac{\kappa}{4\pi} \int_{\mathscr{L}} \frac{(\boldsymbol{s}-\boldsymbol{r})}{|\boldsymbol{s}-\boldsymbol{r}|^3} \mathrm{d}\boldsymbol{s} \tag{85}$$

where $\boldsymbol{r}$ is a point in space and $\boldsymbol{v}_{s0}$ is an arbitrary solution of eqs. (82) and (84) without vortices. It can be found from the boundary conditions. The integral is taken over all vortex lines.

With eq. (85) not only the velocity of an element in the liquid, but also of a point on the vortex can be calculated. In the latter case the integral diverges. This problem is solved by taking into account the finite structure of the vortex core. By comparison with the velocity of a classical vortex ring, the integral can be separated into a local contribution due to the part of the tangle near the point of interest, and a nonlocal contribution due to the rest of the tangle. The velocity of a vortex ring is determined by a parameter β given by $4\pi\beta = \kappa \ln(cR/a_0)$, where R is an average value for the radii of curvature in the vortex tangle, and c is a constant of order one.

Even without calculating the evolution of a vortex tangle, some important properties of the dynamical equilibrium can be derived, if the relative velocity $\boldsymbol{v}_{ns}$ is homogeneous. In the localized induction approximation the equation of motion of the vortex can be written as

$$\frac{\mathrm{d}\boldsymbol{s}}{\mathrm{d}t} = \boldsymbol{v}_{s0} + \beta \boldsymbol{s}' \times \boldsymbol{s}'' + [\alpha - \alpha' \boldsymbol{s}' \times][\boldsymbol{s}' \times (\boldsymbol{v}_{ns} - \beta \boldsymbol{s}' \times \boldsymbol{s}'')], \tag{86}$$

where s is a point on the vortex. The first term yields a uniform translation of the vortex and can be removed by a Galilei transformation. It is possible to define dimensionless length and time scales by introducing the dimensionless length $s_0 = s v_{ns}/\beta$ and the dimensionless time $t_0 = t v_{ns}^2/\beta$. Substitution in eq. (86) yields a dimensionless equation

$$\frac{\mathrm{d}\boldsymbol{s}_0}{\mathrm{d}t_0} = \boldsymbol{s}_0' \times \boldsymbol{s}_0'' + [\alpha - \alpha' \boldsymbol{s}_0' \times][\boldsymbol{s}_0' \times (\boldsymbol{e}_z - \boldsymbol{s}_0' \times \boldsymbol{s}_0'')], \tag{87}$$

where $\boldsymbol{e}_z$ is the unit vector in the z-direction. The z-axis has been chosen in the direction of $\boldsymbol{v}_{ns}$. This equation depends only on α, α' and $\boldsymbol{e}_z$. Hence, if no walls are present, the solution does not depend on the magnitude of the applied velocity v_{ns}. The vortex tangle is homogeneous and oriented along $\boldsymbol{e}_z$.

The density of vortex line length L is given by

$$L = \frac{1}{\Omega}\int_{\mathscr{L}} \mathrm{d}\xi, \tag{88}$$

where the integration is performed over the tangle inside a volume Ω. The line length density equals

$$L = \left(\frac{v_{ns}}{\beta}\right)^2 L_0(\alpha, \alpha'), \tag{89}$$

where the dimensionless vortex length density

$$L_0(\alpha, \alpha') = \frac{1}{\Omega_0}\int_{\mathscr{L}} \mathrm{d}\xi_0 \tag{90}$$

is only a function of α and α'. The integral in eq. (90) is taken in a dimensionless volume Ω_0. Equation (89) shows that L is proportional to v_{ns}^2. In a similar way the average mutual frictional force density $\boldsymbol{F}$ can be calculated.

With the same arguments the dependence of the critical velocity v_c on v_{ns} for flow through a rigid cylindrical tube with diameter D can be determined. In this case the situation of dynamical equilibrium found from eq. (87) is not only a function of α and α', but also of the dimensionless diameter of the tube $v_{ns}D/\beta$. Hence,

$$L = \left(\frac{v_{ns}}{\beta}\right)^2 L_0(\alpha, \alpha', v_{ns}D/\beta) \tag{91}$$

for a certain function L_0. Below the critical velocity $L=0$ in the equilibrium state. Above the critical velocity a turbulent state is present ($L>0$). The function L_0 depends on v_{ns} only through $v_{ns}D/\beta$. Hence,

$$v_c D \approx \text{constant}. \tag{92}$$

Equation (92) has to first order been confirmed by experiment in pure ^{4}He-II (Tough 1982). However, in our derivation it has been neglected that β depends weakly on the local structure of the vortex, as it involves the logarithm of the local radius of curvature. The analysis of Swanson and Donnelly (1985) takes this dependence into account and gives a better agreement with experimental results. Equation (92) has also been verified to first order in the flow of ^{3}He through superfluid ^{4}He (fig. 10). The numerical result recently obtained by Buttke (1987, 1988), which disagrees with eq. (92), has to be rejected on the dimensional grounds given above (Schwarz 1987).

What is still missing is a theoretical derivation of the numerical value of the friction parameter χ introduced in eq. (75). To make up for this deficiency,

one would like to calculate the interaction between a vortex line and one ^{3}He particle, possibly along the lines of the calculation of the ion–vortex interactions (Muirhead et al. 1985). Subsequently, one could calculate the mutual frictional force density. In pure ^{4}He, where the normal fluid consists of only phonons and rotons, it is possible to calculate the interaction between a vortex line and the normal fluid in a semiclassical way (Hillel 1981, Hillel and Vinen 1983). However, the calculation of the mutual frictional force density from first principles in ^{3}He–^{4}He mixtures is an enormous task which has not yet been accomplished.

4.4. *Adiabatic flow in tubes below 250 mK*

In order to study the steady-state flow properties of ^{3}He–^{4}He mixtures we consider a channel, the impedance Z_m, which has a homogeneous cross section with area A. In general, the two components flow with different velocities, as the net ^{4}He transport is assumed to be zero. It is assumed that quadratic terms in the ^{3}He velocity may be neglected, and that the temperature is low enough to neglect thermal phonons and rotons. Furthermore, it will be assumed that the components of the velocities in the radial direction are negligible and that the temperature is uniform in a cross section of the impedance. Terms of order higher than T^2 and $(x-x_0)$ will be neglected. At temperatures below 50 mK, eq. (69) and the low-temperature values given in table 2 hold. Furthermore,

$$\kappa=\kappa_d/T, \quad \text{with} \quad \kappa_d=3\times10^{-4}\ \text{W/m} \tag{93}$$

and

$$V_{m3}=4.26\times10^{-4}\ \text{m}^3/\text{mol}. \tag{94}$$

In this equation $V_{m3}=V_m/x_0$ is the volume of one mole of ^{3}He at concentration x_0. For an impedance of arbitrary, uniform cross section, an impedance factor per unit length ζ, dependent only on the geometry, can be defined such that

$$\frac{dp}{dl}=-\eta\zeta\dot{n}_3 V_{m3} \tag{95}$$

follows from momentum conservation. For Poiseuille flow in a cylindrical tube $\zeta=128/\pi D^4$.

Energy conservation yields

$$\frac{d}{dl}\left\{H_3^{os}\dot{n}_3+\mu_4\dot{n}_4-A\kappa\frac{dT}{dl}\right\}=0. \tag{96}$$

Using eqs. (20) and (24) gives

$$\left\{T\frac{\mathrm{d}}{\mathrm{d}l}\left(\frac{S_\mathrm{m}}{x}\right)+\frac{V_\mathrm{m}}{x}\frac{\mathrm{d}p}{\mathrm{d}l}-\frac{1-x}{x}\frac{\mathrm{d}\mu_4}{\mathrm{d}l}\right\}\dot{n}_3+\frac{\mathrm{d}\mu_4}{\mathrm{d}l}\dot{n}_4-A\frac{\mathrm{d}}{\mathrm{d}l}\left(\kappa\frac{\mathrm{d}T}{\mathrm{d}l}\right)=0. \quad (97)$$

From eqs. (75), (95) and (97) p, T and x can, in principle be calculated as functions of l. However, solution of these equations is complicated because S_m, η, and κ are complicated functions of T and x. However, at low temperatures at concentrations near x_0 one can substitute eqs. (48), (93) and (95), which gives

$$\left\{\tfrac{1}{2}C_\mathrm{d}\frac{\mathrm{d}T^2}{\mathrm{d}l}-\frac{\eta_\mathrm{d}\zeta\dot{n}_3V_{\mathrm{m}3}^2}{T^2}-\frac{1-x_0}{x_0}\frac{\mathrm{d}\mu_4}{\mathrm{d}l}\right\}\dot{n}_3+\frac{\mathrm{d}\mu_4}{\mathrm{d}l}\dot{n}_4-\kappa_\mathrm{d}A\frac{\mathrm{d}}{\mathrm{d}l}\left(\frac{1}{T}\frac{\mathrm{d}T}{\mathrm{d}l}\right)=0. \quad (98)$$

When $\dot{n}_4=0$, eq. (98) reduces to

$$\tfrac{1}{2}C_\mathrm{d}\frac{\mathrm{d}T^2}{\mathrm{d}l}-\frac{\eta_\mathrm{d}\zeta\dot{n}_3V_{\mathrm{m}3}^2}{T^2}-\frac{1-x_0}{x_0}\frac{\mathrm{d}\mu_4}{\mathrm{d}l}-\frac{\kappa_\mathrm{d}}{\dot{n}_3}A\frac{\mathrm{d}}{\mathrm{d}l}\left(\frac{1}{T}\frac{\mathrm{d}T}{\mathrm{d}l}\right). \quad (99)$$

Equation (99) can be put in a dimensionless form by introducing the reduced temperature $t=T/T_0$ and the reduced length $\lambda=l/l_0$, where

$$T_0=\left(\frac{4\kappa_\mathrm{d}\eta_\mathrm{d}V_{\mathrm{m}3}^2A\zeta}{C_\mathrm{d}^2}\right)^{1/6}\approx 3.16\times10^{-4}(A\zeta)^{1/6} \quad (100)$$

and

$$l_0=\left(\frac{2\kappa_\mathrm{d}^2A^2}{C_\mathrm{d}\eta_\mathrm{d}V_{\mathrm{m}3}^2\zeta}\right)^{1/3}\frac{1}{\dot{n}_3}\approx 57.5\frac{A}{\dot{n}_3}(A\zeta)^{-1/3} \quad (101)$$

are the characteristic temperature and length. Substitution in eq. (99) yields

$$-\frac{\mathrm{d}}{\mathrm{d}\lambda}\left(\frac{1}{t}\frac{\mathrm{d}t}{\mathrm{d}\lambda}\right)+\frac{\mathrm{d}t^2}{\mathrm{d}\lambda}-\frac{1}{t^2}-\xi=0, \quad (102)$$

where ξ is a dimensionless parameter equal to

$$\xi=\frac{1-x_0}{x_0}\chi\dot{n}_3^2\left(\frac{4\kappa_\mathrm{d}}{(C_\mathrm{d}\eta_\mathrm{d}V_{\mathrm{m}3}^2A^4\zeta)^2}\right)^{1/3}\approx 1.56\left(\frac{\dot{n}_3}{A}\right)^2(A\zeta)^{-2/3}. \quad (103)$$

The ratio of the last two terms on the left-hand side of eq. (102), ξt^2, is a measure of the ratio of the contributions to the temperature rise due to the viscous force and the mutual frictional force. From the experiments of Wheatley et al. (1971) a value of ξt^2 of the order of 2.5×10^{-4} follows. Hence, the effect of mutual friction is negligible and the viscous force dominates. On

the other hand, in the flow situation of Castelijns et al. (1985) ξt^2 is of the order of 200. This means that in these experiments the viscous force is dominated completely by the mutual frictional force.

Substitution of $d\mu_4/dl=0$ in eq. (99) results in an expression for the mechanical-vacuum model. In this case Wheatley et al. (1968) derived the intrinsic minimum temperature of a ^{3}He circulating dilution refrigerator. Van Haeringen et al. (1979) solved the equation analytically and calculated the temperature profiles in impedances. These results are very useful in designing tubes in dilution refrigerators (van Haeringen 1985).

Equation (102) has been solved numerically in order to calculate the temperature profiles in the case where mutual friction is present (Kuerten et al. 1986a, 1987a, b).

5. Dilution refrigeration

5.1. *Introduction*

The hydrodynamics of ^{3}He moving through ^{4}He at very low temperatures, neglecting mutual friction, has been treated by many authors; see e.g. Frossati (1978). In this section we discuss several ways in which mutual friction affects the operation of dilution refrigerators. The effect can be harmful. However, mutual friction also fulfils an essential condition for the proper and stable operation of dilution machines. This holds for both types of machines: ^{3}He-circulating machines and the so-called ^{4}He-circulating machines.

General introductions in the field of dilution refrigeration can be found in the books of Lounasmaa (1974) and Betts (1976), and in the reviews by Frossati (1978) and Taconis (1982).

5.2. *Limiting mechanisms*

We consider a ^{3}He-circulating dilution refrigerator in which $\dot{n}_3$ moles of pure ^{3}He are circulated per second. The mixing chamber is sketched in fig. 11. The enthalpy balance of the mixing chamber can be written as

$$\dot{Q}+\dot{n}_3 H_3^0(T_i)=\dot{n}_3 H_3^{os}(T_m), \tag{104}$$

where

$$H_3^{os}(T_m)=H_3^{os}(T_m, x_m(T_m)). \tag{105}$$

The total amount of heating power $\dot{Q}$ supplied to the mixing chamber can have several origins:

$$\dot{Q}=\dot{Q}_e+\dot{Q}_\ell+\dot{Q}_d, \tag{106}$$

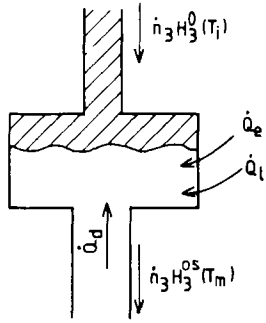

Fig. 11. Schematic drawing of the mixing chamber and the associated enthalpy and heat flows.

where $\dot{Q}_e$ is the heating power resulting from the experiment, $\dot{Q}_\ell$ is the unwanted external heat leak, and $\dot{Q}_d$ represents the heat flowing into the mixing chamber through the *liquid* in the dilute exit tube. In the case that $\dot{Q}_e = \dot{Q}_\ell = 0$, the mixing chamber temperature is determined by several different mechanisms. They will be discussed below.

Even when $\dot{Q}_d = 0$ the mixing chamber temperature at a given $\dot{n}_3$ is determined by the limited surface area of the heat exchangers. The influence of the heat exchanger on the performance of dilution refrigerators is discussed by many authors. We refer especially to the papers by Niinikoski (1976) and Frossati et al. (1977), Frossati (1978).

When the surface area of the heat exchangers is very large the temperature of the mixing chamber tends to be very low (in the 2 mK range) and intrinsic effects will determine the temperature of the mixing chamber, i.e. one can no longer satisfy the condition $\dot{Q}_d = 0$. In the low-temperature region, T_m is determined by a combined result of a large viscosity, a large thermal conductivity ($\dot{Q}_d \neq 0$), and a small cooling power. This effect was first discussed by Wheatley et al. (1968b), and later on in more detail by van Haeringen et al. (1979). The limiting temperature based on the mechanical-vacuum model can be calculated using eq. (102) with $\xi = 0$, and is about $0.7\,T_0$, independent of $\dot{n}_3$.

In general, $\xi \neq 0$; so, also mutual friction has an effect on the limiting value of T_m. The intrinsic minimum T_m calculated with the general expression (102) has a minimum for $\dot{n}_3 = 0$ (this corresponds to $\xi = 0$). The influence of mutual friction on the intrinsic minimum temperature in the single-cycle mode (this is the mode in which the ^{3}He supply to the mixing chamber at the concentrated side is stopped, but the ^{3}He is still extracted at the dilute side) is illustrated in fig. 12.

When the flow impedance at the mixing chamber exit is large, the temperature rise as a result of the dissipation in this tube may prevent further

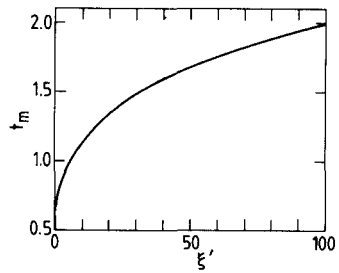

Fig. 12. The calculated minimum (dimensionless) mixing chamber temperature in the single-cycle mode as a function of the mutual friction parameter ξ'. The parameter ξ' is the effective ξ [eq. (103)] for the single-cycle mode, but for all practical purposes one may put $\xi' = \xi$.

cooling of the incoming concentrated ^{3}He flow (de Waele et al. 1984). This mechanism of indirect heating of the mixing chamber via the heat exchangers has been discussed in section 3.3.

It is argued by Geurst et al. (1975) that there should be a jump in the ^{3}He chemical potential at the phase boundary, which drives the ^{3}He across the phase boundary. One would expect that this jump is proportional to the flow rate density at the phase boundary. The jump should lead to an increase in T_m. This interesting effect, which may show up at large flow rate densities, has not been found so far.

5.3. *Mutual friction in ^{3}He-circulating machines*

5.3.1. *Dissipative effects*

For large flow resistances in the dilute channel, the ^{3}He concentration drop can be of the same order as the concentration in the mixing chamber. In that case the ^{3}He concentration in the still will become very low, leading to a high fraction of ^{4}He in the circulated mixture (compare curve 4 in fig. 5). In many cases the point where the concentration drop in the dilute channel is approximately equal to the concentration in the mixing chamber shows up in the plot of the total flow rate versus still heating power as a kink (Castelijns et al. 1985).

For a single cylindrical tube with diameter D, carrying a Poiseuille flow of ^{3}He, the product $A\zeta = 32/D^2$. In this case eqs. (100) and (103) can be written as

$$D = 1.78 \times 10^{-10}/T_0^3 \tag{107}$$

and

$$\xi = 0.25 \dot{n}_3^2 / D^{2/3}. \tag{108}$$

Equation (107) gives the order of magnitude of the diameter D of the dilute channel in the exit of the mixing chamber reaching its intrinsic low-temperature limit T_0. For $T_0 = 2$ mK, eq. (107) results in $D = 22$ mm. For $\dot{n}_3 = 5$ mmol/s eq. (108) gives $\xi = 0.16$. Since $t \approx 1$ near the intrinsic limit, one obtains $\xi t^2 \approx 0.16$, so the effect of mutual friction on the solution of eq. (102) is small. This is mainly due to the large viscosity at very low temperatures. However, when D is determined by eq. (107) with higher T_0, then the mutual friction will soon dominate the viscous effects. Fortunately, eq. (107) leads to very small diameters in the high-temperature regions, and it is quite easy to make the tube diameters somewhat larger, thereby reducing the effects of mutual friction and viscosity.

In general, mutual friction does not necessarily degrade the performance of dilution refrigerators, but in machines which are *critically* designed according to the criteria of the mechanical-vacuum model, problems can be expected. As was demonstrated by Castelijns et al. (1985), a superleak shunt across a flow channel in which mutual friction causes problems can help to overcome the harmful effects.

5.3.2. *Stabilizing effects of mutual friction*

In the discussion so far it is shown that mutual friction has a degrading effect on many aspects of dilution refrigerators. However, mutual friction has also a very good influence on the operation of the machine. It is essential for their (stable) operation. As put forward by Wheatley et al. (1971) the temperature gradients are relatively large in the regions around the still and the 1 K bath. The resulting osmotic pressure gradients exert forces on the ^{4}He component which are larger than the forces from the ordinary pressure gradient at the concentrated side. This drives the ^{4}He to regions of high temperatures and high ^{3}He concentrations. An eventual superfluid column (plug) in these regions cannot be removed.

If mutual friction would be absent, the ^{4}He in the concentrated channel of the machine would not leave the channel during start up. For similar reasons, during continuous operation, ^{4}He would move from the mixing chamber into the concentrated channel via the superfluid ^{4}He film, or stay there after entering the channel as the (small) ^{4}He fraction of the circulating mixture.

The presence of a superfluid plug would lead to dilution of ^{3}He (and cooling) in warm regions, and demixing (and heating) in the cold spots. For example, cooling would take place in the concentrated channel near the still, and heating in the heat exchangers. This would prevent the proper operation of the machine. Hence, a mechanism driving the ^{4}He out of the concentrated channel is necessary. Mutual friction is the only known force which can balance the osmotic forces. Therefore, it must play an essential role in this process.

5.4. *Mutual friction in ^{4}He-circulating machines*

In ^{4}He-circulating refrigerators (see e.g. Satoh et al. 1987) ^{4}He is used to drive the circulation of ^{3}He. Especially, in this type of machines mutual friction plays an essential role. In this discussion we assume that the dilute phase flows from the mixing chamber towards the demixing chamber in the form of droplets (Griffioen et al. 1986). This does not affect the general conclusion. Figure 13 is a schematic drawing of the process we have in mind.

In contrast to what is suggested by the name, it is not the ^{4}He flow which determines the cooling power, but the ^{3}He flow resulting from it. The ^{3}He in the dilute phase is dragged along with the ^{4}He in the droplets. If there would be no mutual friction between ^{3}He and ^{4}He, the latter would move to the demixing chamber without taking the ^{3}He along. This can be understood as follows: there is a temperature gradient in the tube connecting the mixing chamber (typically at 10 mK) with the demixing chamber (around a few hundred mK). As the droplet moves in this tube, there is also a temperature gradient in the droplet, with a corresponding gradient of the osmotic pressure. This would lead to an acceleration of ^{4}He towards the warm end of the droplet, accompanied by a mixing (and cooling) at the warm end of the droplet, and a demixing (and heating) at the cold end. Near the mixing chamber the heating of the droplets leaving the mixing chamber would balance the cooling power. In essence, ^{4}He would move towards the demi-

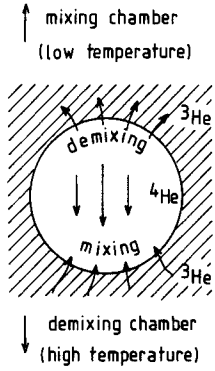

Fig. 13. Schematic drawing of a droplet of a ^{3}He–^{4}He solution in the dilute phase falling through the concentrated phase (hatched region) in a tube connecting the mixing chamber and the demixing chamber of a ^{4}He-circulating dilution refrigerator. As a result of the temperature gradient in the tube, there is a T-gradient in the droplet. This leads to a gradient in the osmotic pressure in the droplet which drives the superfluid ^{4}He from the cold end (top) towards the warm end (bottom), resulting in demixing at the cold end and mixing at the warm end.

xing chamber without dragging ^{3}He along and, hence, without producing cooling in the mixing chamber.

Due to the mutual friction, the difference in ^{3}He and ^{4}He velocities is limited. This is comparable to the cooling mechanism in the so-called vortex cooler (see e.g. Okuyama 1987), where the mutual friction between the superfluid and the normal component leads to the proper operation of the device.

6. Discussion

6.1. *Comparison between ^{4}He-II and ^{3}He–^{4}He-II mixtures*

In this section a comparison will be made between the hydrodynamics of pure ^{4}He-II and of ^{3}He–^{4}He-II mixtures. The macroscopic description of the hydrodynamics of pure ^{4}He-II is based on the two-fluid model. The mutual friction between the normal and the superfluid components is presumably caused by the interaction of the normal component with quantized vortices. The state of superfluid turbulence is investigated under various experimental conditions such as temperature, geometry and velocities (Tough 1982, Glaberson and Donnelly 1985). For cylindrical capillaries there are three flow regimes. Below a first critical value of the relative velocity, there is no mutual friction. If that critical velocity is exceeded, mutual friction appears, but the resulting state is inhomogeneous and anisotropic (TI). Furthermore, the transition between the laminar and turbulent state exhibits hysteresis. At still higher velocities a second transition occurs to a state of homogeneous and isotropic turbulence (TII). This state is described reasonably well by the motion of a vortex tangle as numerically simulated by Schwarz.

Mixtures of ^{3}He and superfluid ^{4}He can also be regarded as a mixture of two components, with the normal component consisting of the ^{3}He plus the normal part of the ^{4}He. The mutual friction between ^{3}He and ^{4}He is not caused by the friction of ^{3}He with the normal component of the ^{4}He, because it is also present at temperatures where thermal phonons and rotons are absent. In the hydrodynamics of ^{3}He–^{4}He solutions, critical velocities play a role which are quite similar to the critical velocities in pure ^{4}He-II. There also is an indication that there is a second critical velocity above which the turbulence is fully developed. It seems that the ratio of the two critical velocities (approximately 2) is the same as in pure ^{4}He. In contrast to the situation in pure superfluid ^{4}He, the critical velocities are independent of temperature in the temperature range of the experiments ($10 < T < 250$ mK).

The fact that the behaviour of ^{3}He–^{4}He mixtures is so similar to ^{4}He-II is surprising. Mutual friction is caused by the interaction between excitations

and quantized vortices, which is determined by quantum mechanics. The excitations in pure superfluid ^{4}He (phonons and rotons) obey Bose statistics. On the other hand, the excitations in mixtures are the ^{3}He quasiparticles, which obey Fermi statistics. Therefore, one would expect a difference in flow properties. The calculation of the strength of the ^{3}He–vortex interaction from the many-particle interactions is one of the basic problems in the field of ^{3}He–^{4}He hydrodynamics.

In ^{3}He–^{4}He mixtures the temperature and density can be varied independently. This offers some advantage over pure ^{4}He. For example, in pure ^{4}He it appears that the critical velocity is temperature-dependent, whereas in mixtures the critical velocity seems to be independent of temperature. This suggests that the temperature dependence in pure ^{4}He is mainly due to the variation of the density of the normal component.

The similarity between the properties of pure ^{4}He-II and ^{3}He–^{4}He-II mixtures makes it also possible to apply the simulations of the motion of quantized vortices in pure ^{4}He to mixtures. Schwarz derived an expression for the frictional force exerted by the normal fluid on a vortex. This expression contains two parameters which depend on the microscopic interactions between the normal fluid and a vortex line. If these parameters are known for mixtures, Schwarz's results can be applied to mixtures.

6.2. *Thermodynamics*

Since the mid-seventies the measurements of the thermodynamic properties of mixtures have been extended by precise measurements of the specific heat and the velocity of second sound. It is remarkable that this accuracy in the measurements has not led to a precise knowledge of the effective mass (Bowley 1988). The specific heat data of Greywall were refitted several times and, in fact, could be fit by the parameters showing up in various models. The specific heat measurements of Owers–Bradley are analyzed in terms of the nearly ideal Fermi gas, but higher-order terms in the nonparabolic excitation spectrum play an important role; so, a consistent higher-order analysis is necessary, i.e. terms of 6th (or even higher) order of the wave vector in the quasiparticle excitation spectrum should be taken into account.

In this review we have chosen a systematic fourth-order approximation. In principle, higher-order approximations can be derived in an analogous way but lead to tedious calculations and complicated expressions. Moreover, one may wonder whether the introduction of new fitting parameters will lead to less uncertainty in the description of the system.

In sect. 2.3 we have emphasized that the separation of the specific heat into a Fermi quasiparticle contribution and a ^{4}He contribution may be an

oversimplification. If this is so it may have consequences for the parameters derived from models of the ^{3}He–^{4}He solutions.

6.3. *Hydrodynamics*

At present, the hydrodynamic properties in the temperature range from 10–250 mK are fairly well described. At temperatures above 500 mK phonons and rotons will affect the ^{3}He hydrodynamics. There have been a few investigations in the temperature range where phonons and rotons play a role, but the transition region from the low-temperature range, where phonons and rotons can be neglected, to the high-temperature range has not been investigated.

The mesoscopic description in terms of superfluid turbulence is in full development at the moment. One may hope that the calculations will clarify the origin of the critical velocities. One of the fields for future research is the study of time-dependent effects (fluctuations) which accompany the transitions in the critical velocity regions.

Below 10 mK interesting effects may show up in the ballistic regime (Guénault and Pickett 1984), i.e. when the quasiparticle mean free path is of the order of the average vortex–line distance, or when the quasiparticle mean free path is of the order of the tube diameter. It is speculated that in the very low temperature regime mixtures can be superfluid (see Ishimoto et al. 1987 and the references therein). Of course, this would open the possibility to study the interesting properties of a mixture of two superfluids, one of which can be varied over a large range of densities. Unfortunately, at present there are no indications that this exciting temperature range has been entered yet.

Acknowledgements

We thank the members of the Low Temperature Physics Group of the Eindhoven University of Technology for reading the manuscript and their patient cooperation during the preparation of this review. Especially, we thank J. Zeegers for supplying his data on the ^{3}He–^{4}He flow properties prior to publication.

References

Abraham, B.M., D.W. Osborne and B. Weinstok, 1950, Phys. Rev. **80**, 366.
Abraham, B.M., O.G. Brandt, Y. Eckstein, J. Munarin and G. Baym, 1969, Phys. Rev. **188**, 309.
Adamenko, I.N., and É.Ya. Rudavskii, 1987, Sov. J. Low Temp. Phys. **13**, 1.

Adamenko, I.N., É.Ya. Rudavskii, V.I. Tsyganok and V.K. Chagovets , 1988, J. Low Temp. Phys. **71**, 261.
Alvares, L.W., and R. Cornog, 1939, Phys. Rev. **56**, 379, 613.
Anderson, A.C., D.O. Edwards, W.R. Roach, R.E. Sarwinski and J.C. Wheatley, 1966, Phys. Rev. Lett. **17**, 376.
Ardron, M.R., P.G.J. Lucas and A. Tyler, 1987, Proc. 18th Int. Conf. on Low Temperature Physics, Kyoto, Jpn. J. Appl. Phys. **26**, Suppl. 26-3, p. 77.
Armitage, J.G.M., and I.E. Farquhar, 1975, The Helium Liquids (Academic Press, London).
Bardeen, J., G. Baym and D. Pines, 1966, Phys. Rev. Lett. **17**, 372.
Bardeen, J., G. Baym and D. Pines, 1967, Phys. Rev. **156**, 207.
Bashkin, E.P., and A.E. Meyerovich, 1981, Adv. Phys. **30**, 1.
Baym, G., and C. Pethick, 1978, The Physics of Liquid and Solid Helium, part 2, eds K.H. Benneman and J.B. Ketterson (Wiley, New York) ch. 2.
Beenakker, J.J.M., and K.W. Taconis, 1955, Progress in Low Temperature Physics, Vol. I, ed. C.J. Gorter (North-Holland, Amsterdam) ch. VI.
Betts, D.S., 1976, Refrigeration and Thermometry below One Kelvin (Sussex University Press, Brighton, UK).
Bloodworth, T.J., M.R. Ardron and P.G.J. Lucas, 1987, Proc. 18th Int. Conf. on Low Temperature Physics, Kyoto, Jpn. J. Appl. Phys. **26**, Suppl. 26-3, p. 59.
Bowley, R.M., 1985, J. Low Temp. Phys. **61**, 291.
Bowley, R.M., 1988, J. Low Temp. Phys. **71**, 319.
Brubaker, N.R., D.O. Edwards, R.E. Sarwinski, P. Seligmann and R.A. Sherlock, 1970, Phys. Rev. Lett. **25**, 715; J. Low Temp. Phys. **3**, 619.
Brucker, H., Y. Disatnik and R. Meyuhas, 1976, J. Low Temp. Phys. **24**, 193.
Buttke, T.F., 1987, Phys. Rev. Lett. **59**, 2117.
Buttke, T.F., 1988, J. Comput. Phys. **76**, 301.
Castelijns, C.A.M., J.G.M. Kuerten, A.T.A.M. de Waele and H.M. Gijsman, 1985, Phys. Rev. B **32**, 2870.
Chocholacs, H.C., R.M. Mueller, J.R. Owers-Bradley, Ch. Buchal, M. Kubota and F. Pobell, 1984, Proc. 17th Int. Conf. on Low Temperature Physics, eds U. Eckern, A. Schmid, W. Weber and H. Wühl (North-Holland, Amsterdam) p. 1247.
Cohen, E.G.D., and J.M.J. van Leeuwen, 1960, Physica **26**, 1171.
Coops, G.M., A.T.A.M. de Waele and H.M. Gijsman, 1979, Cryogenics **19**, 659.
Coops, G.M., A.T.A.M. de Waele and H.M. Gijsman, 1982, Phys. Rev. B **25**, 4879.
Corruccini, L.R., 1984, Phys. Rev. B **30**, 3735.
Dalfovo, F., and S. Stringari, 1988, J. Low Temp. Phys. **71**, 331.
Das, P., R. de Bruyn Ouboter and K.W. Taconis, 1964, Proc. IXth Int. Conf. on Low Temperature Physics, Columbus, Ohio, eds J.G. Daunt, D.O. Edwards, F.J. Milford and M. Yagub (Plenum Press, New York) p. 1253.
De Bruyn Ouboter, R., and C.N. Yang, 1987, Physica B **144**, 127.
De Bruyn Ouboter, R., K.W. Taconis, C. le Pair and J.J.M. Beenakker, 1960, Physica **26**, 853.
De Groot, S.R., and P. Mazur, 1962, Nonequilibrium Thermodynamics (North-Holland, Amsterdam).
De Waele, A.T.A.M., and J.G.M. Kuerten, 1989, Physica B **160**, 143.
De Waele, A.T.A.M., J.C.M. Keltjens, C.A.M. Castelijns and H.M. Gijsman, 1983, Phys. Rev. B **28**, 5350.
De Waele, A.T.A.M., J.C.M. Keltjens, C.A.M. Castelijns and H.M. Gijsman, 1984, Adv. Cryogenic Eng. **29**, 565.
Devreese, J.T., L.F. Lemmens and F. Brosens, 1989, to be published.
Disatnik, Y., and H. Brucker, 1972, J. Low Temp. Phys. **7**, 491.

Donnelly, R.J., 1987, Phys. Today **40**, 23.
Ebner, C., 1967, Thesis (University of Illinois) unpublished.
Ebner, C., and D.O. Edwards, 1971, Phys. Rep. C **2**, 77.
Ecke, R.E., H. Hauke and J.C. Wheatley, 1987, Phys. Rev. Lett. **58**, 499; Can. J. Phys. **65**, 1322.
Edwards, D.O., and J.G. Daunt, 1961, Phys. Rev. **124**, 640.
Edwards, D.O., D.F. Brewer, P. Seligmann, M. Skertic and M. Yaqub, 1965, Phys. Rev. Lett. **15**, 773.
Ellis, T., and P.V.E. McClintock, 1985, Philos. Trans. R. Soc. London A **315**, 259.
Esel'son, B.N., V.A. Slyusarev, V.Il. Sobolev and M.A. Strzhemechnyi, 1976, Sov. J. Low Temp. Phys. **2**, 207.
Fabrochini, A., 1986, Phys. Rev. B **33**, 6057.
Fetter, A.L., 1982, Phys. Rev. B **26**, 1164.
Feynman, R.P., 1955, Progress in Low Temperature Physics, Vol. 1, ed. C.J. Gorter (North-Holland, Amsterdam) ch. II.
Frossati, G., 1978, J. Phys. Colloq. (France) **39**, C6 Suppl. 8, 1578.
Frossati, G., H. Godfrin, B. Hebral, G. Schumacher and D. Thoulouze, 1977, Physics at Ultra low Temperatures, in: Proc. Int. Symp., Hakone, ed. P. Sugawara (Physical Society of Japan, Tokyo) p. 205.
Fujii, I., A.J. Ikushima, K. Kaneko and M. Suzuki, 1986, J. Low Temp. Phys. **63**, 535.
Fukuyama, H., I. Kurikawa, H. Ishimoto and S. Ogawa, 1988, Techn. Rep. Institute of Solid State Physics, University of Tokyo, Ser. A, No. 2046.
Geurst, J.A., F.A. Staas and W. van Haeringen, 1975, Phys. Lett. A **55**, 251.
Ghozlan, A.C., and E.J.A. Varoquaux, 1969, Phys. Lett. A **30**, 426.
Ghozlan, A.C., and E.J.A. Varoquaux, 1979, Ann. Phys. (France) **4**, 239.
Glaberson, W.I., and R.J. Donnelly, 1985, Progress in Low Temperature Physics, Vol. 8, ed. D.F. Brewer (North-Holland, Amsterdam) ch. 1.
Gorter, C.J., and J.H. Mellink, 1949, Physica **15**, 185.
Greywall, D.S., 1978a, Phys. Rev. Lett. **41**, 177.
Greywall, D.S., 1978b, Phys. Rev. B **18**, 2127.
Greywall, D.S., 1979, Phys. Rev. B **20**, 2643.
Greywall, D.S., 1982, Phys. Rev. B **27**, 2747.
Greywall, D.S., 1985, Phys. Rev. B **31**, 2675.
Greywall, D.S., 1986, Phys. Rev. B **33**, 7520.
Greywall, D.S., and M.A. Paalanen, 1981, Phys. Rev. Lett. **46**, 1292.
Griffioen, W., H.W. Jentink and R. de Bruyn Ouboter, 1986, Physica B **141**, 137.
Guénault, A.M., and G.R. Pickett, 1984, Physica B+C **126**, 260.
Guggenheim, E.A., 1967, Thermodynamics (North-Holland, Amsterdam).
Hendry, P.C., and P.V.E. McClintock, 1987, Cryogenics **27**, 131.
Hendry, P.C., N.S. Lawson, P.V.E. McClintock, C.D.H. Williams and R.M. Bowley, 1988, Phys. Rev. Lett. **60**, 604.
Hillel, A.J., 1981, J. Phys. C **14**, 4027.
Hillel, A.J., and W.F. Vinen, 1983, J. Phys. C **16**, 3267.
Hsu, W., and D. Pines, 1985, Phys. Rev. B **32**, 7179.
Huang, K., 1987, Statistical Mechanics (Wiley, New York).
Husson, L.P.J., C.E.D. Ouwerkerk, A.L. Reesink and R. de Bruyn Ouboter, 1983, Physica B **122**, 183.
Ishimoto, H., H. Fukuyama, N. Nishida, Y. Miura, Y. Takano, T. Fukuda, T. Tazaki and S. Ogawa, 1987, Proc. 18th Int. Conf. on Low Temperature Physics, Kyoto, Jpn. J. Appl. Phys. **26**, 67.
Jackson, H.W., 1982, Phys. Rev. B **26**, 66; B **28**, 183.
Jackson, J.D., 1975, Classical Electrodynamics (Wiley, New York) ch. 5.

Kamerlingh Onnes, H., 1908, Commun. Phys. Lab., Leiden, No. 108, Proc. R. Acad. Amsterdam **11**, 168.
Karnatsevich, L.V., I.V. Bogoyavlenskii and G. Konareva, 1984, Sov. J. Low Temp. Phys. **10**, 300.
Keller, W.E., 1969, Helium-3 and Helium-4 (Plenum Press, New York).
Khalatnikov, I.M., 1965, An Introduction to the Theory of Superfluidity (W.A. Benjamin, New York).
Kierstead, H.A., 1976, J. Low Temp. Phys. **24**, 193.
Krotscheck, E., M. Saarela and J.L. Epstein, 1988, Phys. Rev. Lett. **61**, 1728.
Kuenhold, K.A., D.B. Crum and R.E. Sarwinski, 1972, Phys. Lett. A **41**, 13.
Kuerten, J.G.M., 1987b, Thesis (University of Technology, Eindhoven) unpublished.
Kuerten, J.G.M., C.A.M. Castelijns, A.T.A.M. de Waele and H.M. Gijsman, 1985a, Physica B **128**, 197.
Kuerten, J.G.M., C.A.M. Castelijns, A.T.A.M. de Waele and H.M. Gijsman, 1985b, Cryogenics **25**, 419.
Kuerten, J.G.M., C.A.M. Castelijns, A.T.A.M. de Waele and H.M. Gijsman, 1986a, Phys. Scr. T **13**, 109.
Kuerten, J.G.M., C.A.M. Castelijns, A.T.A.M. de Waele and H.M. Gijsman, 1986b, Phys. Rev. Lett. **56**, 2288.
Kuerten, J.G.M., J. Zeegers, A.T.A.M. de Waele and H.M. Gijsman, 1987a, Proc. 18th Int. Conf. on Low Temperature Physics, Kyoto, Jpn. J. Appl. Phys. **26**, Suppl. 26-3, p. 29.
Laheurte, J.P., J.C. Noiray and J.P. Romagnan, 1987, Phys. Lett. A **123**, 101.
Landau, J., and R.L. Rosenbaum, 1973, J. Low Temp. Phys. **11**, 483.
Landau, J., J.T. Tough, N.R. Brubaker and D.O. Edwards, 1970, Phys. Rev. A **2**, 2472.
Landau, L.D., 1941, J. Phys. USSR **5**, 71.
Landau, L.D., and I. Pomeranchuk, 1948, Dokl. Akad. Nauk. SSR **59**, 668.
Lea, M.J., P.W. Retz and P. Fozooni, 1987, J. Low Temp. Phys. **66**, 325.
Lin, C.C., 1963, Liquid Helium, ed. G. Careri (Academic Press, New York) p. 93.
London, H., 1951, Proc. Int. Conf. on Low Temperature Physics, Oxford, 1951 (Clarendon Laboratory, Oxford, UK) p. 157.
London, H., G.R. Clarke and E. Mendoza, 1962, Phys. Rev. **128**, 1992.
London, H., H. Berks, D. Phillips and G.P. Thomas, 1968, Proc. 11th Int. Conf. on Low Temperature Physics, St. Andrews, eds J.F. Allen, D.M. Finlayson and D.M. McCall, p. 649.
Lounasmaa, O.V., 1974, Experimental Principles and Techniques Below 1 K (Academic Press, New York).
Mazur, P., and I. Prigogine, 1951, Physica **17**, 680.
Meyer, H., 1988, J. Low Temp. Phys. **70**, 219.
Meyerovich, A.E., 1987, Progress in Low Temperature Physics, Vol. XI, ed. D.F. Brewer (North-Holland, Amsterdam) ch. I.
Mudde, R.F., 1989, Thesis (University of Leiden, Leiden) unpublished.
Mudde, R.F., and H. van Beelen, 1987, Proc. 18th Int. Conf. on Low Temperature Physics, Kyoto, Jpn. J. Appl. Phys. **26**, Suppl. 26-3, p. 103.
Muirhead, C.M., W.F. Vinen and R.J. Donnelly, 1985, Proc. R. Soc. A **402**, 225.
Neganov, B.S., N. Borisov and M. Liburg, 1966, Sov. Phys.-JETP **23**, 959.
Niinikoski, T.O., 1971, Nucl. Instrum. & Methods **97**, 95.
Niinikoski, T.O., 1976, Proc. ICEC 6 (IPS Science and Technical Press, Guildford, UK) p. 102.
Okuyama, M., T. Satoh and T. Satoh, 1987, Proc. 18th Int. Conf. on Low Temperature Physics, Kyoto, Jpn. J. Appl. Phys. **26**, Suppl. 26-3, p. 101.
Onsager, L., 1949, Nuovo Cimento **6**, Suppl. 2, 249.
Owers-Bradley, J.R., P.C. Main, G.J. Batey, R.J. Church and R.M. Bowley, 1987, Jpn. J. Appl. Phys. **26**, 15.

Owers-Bradley, J.R., P.C. Main, G.J. Batey, R.J. Church and R.M. Bowley, 1988, J. Low Temp. Phys. **72**, 201.
Pang, T., 1988, Phys. Rev. Lett. **61**, 849.
Papoular, M., and J.P. Romagnan, 1987, Europhys. Lett. **3**, 839.
Peshkov, 1968, Sov. Phys.-Usp. **11**, 209.
Pfitzer, M., 1985, J. Low Temp. Phys. **61**, 141.
Pogorelov, L.A., B.N. Esel'son, O.S. Nosovitskaya and V.Il. Sobolev, 1979, Sov. J. Low Temp. Phys. **5**, 40.
Polturak, E., and R. Rosenbaum, 1981, J. Low Temp. Phys. **43**, 477.
Pomeranchuk, I.J., 1949, Zh. Eksp. & Teor. Fiz. **19**, 42.
Prigogine, I., and P. Mazur, 1951, Physica **17**, 661.
Radebaugh, R., 1967, NBS Technical Note 362 (National Bureau of Standards, Gaithersburg, VA).
Rent, L.S., and I.S. Fisher, 1969, Sov. Phys.-JETP **28**, 375.
Ruvalds, J., and T. Regge, 1978, Quantum Liquids (North-Holland, Amsterdam).
Satoh, N., T. Satoh, T. Ohtsuka, N. Fukuzawa and N. Sato, 1987, J. Low Temp. Phys. **67**, 195.
Schwarz, K.W., 1978, Phys. Rev. B **18**, 245.
Schwarz, K.W., 1982, Phys. Rev. Lett. **49**, 283.
Schwarz, K.W., 1985, Phys. Rev. B **31**, 5782.
Schwarz, K.W., 1987, Phys. Rev. Lett. **59**, 2118.
Seligmann, P., D.O. Edwards, R.E. Sarwinski and J.T. Tough, 1969, Phys. Rev. **181**, 415.
Singh, K.K., 1988, Phys. Rev. B **37**, 419.
Sobolev, V.Il., B.N. Edelson, D.S. Noviskaya and L.A. Pogorelov, 1979, Sov. J. Low Temp. Phys. **5**, 269.
Sridhar, R., and A. Shanthi, 1987, Proc. 18th Int. Conf. on Low Temperature Physics, Kyoto, Jpn. J. Appl. Phys. **26**, Suppl. 26-3, p. 41.
Stoner, E.C., 1938, Philos. Mag. **25**, 899.
Swanson, C.E., and R.J. Donnelly, 1985, J. Low Temp. Phys. **61**, 363.
Szprynger, A., 1982, J. Low Temp. Phys. **49**, 135.
Taconis, K.W., 1982, Physica B **109&110**, 1753.
Taconis, K.W., and R. de Bruyn Ouboter, 1964, Progress in Low Temperature Physics, Vol. IV, ed. C.J. Gorter (North-Holland, Amsterdam) ch. II.
Tough, J.T., 1982, Progress in Low Temperature Physics, Vol. VIII, ed. D.F. Brewer (North-Holland, Amsterdam) p. 133.
Valles Jr, J.M., R.H. Higley, R.B. Johnson and R.B. Hallock, 1988, Phys. Rev. Lett. **60**, 428.
Van der Boog, A.G.M., L.P.J. Husson and H.C. Kramers, 1978, Phys. Lett. A **66**, 305.
Van der Boog, A.G.M., L.P.J. Husson, Y. Disatnik and H.C. Kramers, 1981a, Physica B **104**, 285, 303.
Van der Boog, A.G.M., Y. Disatnik and H.C. Kramers, 1981b, Physica B **104**, 316.
Van der Zeeuw, H.C.M., L.P.J. Husson, M. Durieux and R. de Bruyn Ouboter, 1984, Proc. 17th Int. Conf. on Low Temperature Physics, eds U. Eckern, A. Schmid, W. Weber and H. Wühl (North-Holland, Amsterdam) p. 1245.
Van Haeringen, W., 1985, Cryogenics **20**, 153.
Van Haeringen, W., F.A. Staas and J.A. Geurst, 1979, Philips J. Res. **34**, 107.
Varoquaux, E.J.A., 1971, Thesis (Orsay).
Vinen, W.F., 1957, Proc. R. Soc. A **242**, 493.
Watson, G.W., J.D. Reppy and R.C. Richardson, 1969, Phys. Rev. **188**, 384.
Wheatley, J.C., 1970, Progress in Low Temperature Physics, Vol. VI, ed. C.J. Gorter (North-Holland, Amsterdam) ch. III.
Wheatley, J.C., O.E. Vilches and R.T. Johnson, 1968, Physics **4**, 1.

Wheatley, J.C., J.C. Rapp and R.T. Johnson, 1971, J. Low Temp. Phys. **4**, 1.
Wiegers, S.A.J., R. Jochemsen, C.C. Kranenburg and G. Frossati, 1988, J. Low Temp. Phys. **71**, 69.
Wilks, J., 1967, The Properties of Liquid and Solid Helium (Clarendon Press, Oxford).
Zeegers, J., J.G.M. Kuerten, A.T.A.M. de Waele and H.M. Gijsman, 1987, Proc. 18th Int. Conf. on Low Temperature Physics, Kyoto, Jpn. J. Appl. Phys. **26**, Suppl. 26-3, p. 63.
Zeegers, J., J.G.M. Kuerten, A.T.A.M. de Waele and H.M. Gijsman, 1989, to be published.